

LUC-2-1682 Anthony Wayne Bridge

Main Cable Long Term Health Monitoring



Prepared by:
Kyle Layton & Douglas Nims

Prepared for:
The Ohio Department of Transportation,
Office of Statewide Planning &
Research

State Job Number: 427318

January, 2014

Final Report



Technical Report Documentation Page

1. Report No. FHWA/OH-2014/1		2. Government Accession No.		3. Recipient's Catalog No.	
4. Title and Subtitle LUC-2-1682 Anthony Wayne Bridge Main Cable Long Term Health Monitoring				5. Report Date January 2014	
				6. Performing Organization Code	
7. Author(s) Kyle Layton, Douglas Nims				8. Performing Organization Report No.	
9. Performing Organization Name and Address University of Toledo 2801 W. Bancroft Toledo, Ohio 43606				10. Work Unit No. (TRAIS)	
				11. Contract or Grant No. 427318	
12. Sponsoring Agency Name and Address Ohio Department of Transportation 1980 West Broad Street Columbus, Ohio 43223				13. Type of Report and Period Covered	
				14. Sponsoring Agency Code	
15. Supplementary Notes					
16. Abstract In preparation for a large rehabilitation project on the Anthony Wayne Bridge (AWB), the Ohio Department of Transportation has expressed interest in evaluating monitoring and protection strategies which may extend the life of the AWB. This study was proposed and performed in line with this goal. Corrosion of the main cable was identified as the driving mechanism for the aging of suspension bridges. Experiments were performed in order to determine whether or not the existing acoustic monitoring system on the AWB could be used to readily identify active corrosion. Results from laboratory testing show that use of acoustic emission to detect corrosion is possible and promising; however, field experiments indicate that additional tests are needed to determine the practicality of identifying corrosion in the field. The upcoming bridge closure will provide a great opportunity for researchers to more closely examine this possibility. In addition, this report includes literature investigation into other state-of-the-art corrosion monitoring and protection strategies including an internal sensor array, the magnetic main flux method for wire inspection, and cable dehumidification.					
17. Keywords Bridges, suspension, main cable, corrosion, aging				18. Distribution Statement No restrictions. This document is available to the public through the National Technical Information Service, Springfield, Virginia 22161	
19. Security Classification (of this report) Unclassified		20. Security Classification (of this page) Unclassified		21. No. of Pages	
				22. Price	

Form DOT F 1700.7 (8-72)

Reproduction of completed pages authorized

LUC-2-1682 Anthony Wayne Bridge

Main Cable Long Term Health Monitoring

Prepared by:

Kyle Layton and Douglas Nims

University of Toledo

January, 2014

Prepared in cooperation with the Ohio Department of Transportation
and the U.S. Department of Transportation, Federal Highway Administration

The contents of this report reflect the views of the authors who are responsible for the facts and the accuracy of the data presented herein. The contents do not necessarily reflect the official views or policies of the Ohio Department of Transportation or the Federal Highway Administration. This report does not constitute a standard, specification, or regulation.

Acknowledgments

The authors would like to thank Mike Loeffler, Doug Rogers and Lloyd Welker, whom comprised the Technical Panel members on this project, for their continual guidance and eagerness to work with the research team along the way.

Thank you also to Richard Gostautas and Terry Tamutus of Mistras Group, Inc. Their time, patience and expertise were sincerely appreciated throughout this project.

They authors also gratefully acknowledge the assistance of Mr. Dyab Khazem, of Parsons Transportation Group, Dr. Raimondo Betti, of Columbia University, and Dr. Bojidar Yanev, of NYC DOT.

Thank you also to Kushal Niroula, who provided support and insight during corrosion experiments and data analysis.

Table of Contents

Cover	1
Form DOT F 1700.7	2
Title Page.....	3
Acknowledgements.....	4
Table of Contents.....	5
List of Figures	6
List of Tables.....	6
1.0 Introduction	7
1.1 Description of bridge	8
1.2 Recent Monitoring & Inspections.....	8
1.3 Background on AE	9
2.0 Research Objectives.....	10
3.0 General Description of Research.....	11
4.0 Research Results & Findings.....	12
4.1 Corrosion Monitoring Experiments	12
4.1.1 Experimental Background.....	12
4.1.2 Chemistry of Corrosion	12
4.1.3 Development of the Experimental Program.....	13
4.1.4 Experimental Results & Discussion	15
4.2 Findings from Review of Monitoring and Preservation Technologies.....	23
4.2.1 Internal Sensor Technology	23
4.2.2 Magnetic Main Flux Method.....	26
4.2.3 Dehumidification	28
5.0 Conclusions & Recommendations	32
5.1 Summary of Current Condition.....	32
5.2 Rehabilitation and Advanced Inspection Cost vs. Reliability Estimates	32
5.3 Best Practices Recommendation for the Anthony Wayne.....	32
5.4 Future Research.....	33
6.0 Recommendations for Implementation of Research Findings	34
7.0 Bibliography	35
Appendices	37
Appendix A: Sample Data Sheets from Corrosion Testing.....	38
Appendix B: Internal Sensors Product Specifications	41
Appendix C: Quote from CTNA for MMFM Inspection of AW.....	45

List of Figures

Figure 1: Elevation drawing of the north and south cables on the Anthony Wayne Bridge.....	7
Figure 2: AE waveform features [Gostautas et al., 2012]	9
Figure 3: Schematic of A sources during corrosion, SCC and corrosion fatigue processes [Yuyama, 2002].....	12
Figure 4: Corrosion cell with wires	14
Figure 5: Set-up for laboratory corrosion cell testing	15
Figure 6: Hits vs. Time for C3-NW-SS3-2	15
Figure 7: Hits vs. Time for C3-UG-SS3-2	15
Figure 8: Hits vs. Time for C3-G-SS3-2	15
Figure 9: Visual of cumulative corrosion for each cell after completion of laboratory testing	17
Figure 10: Hits vs. time for C3-UG-SS3-1	18
Figure 11: Set-up for mock cable band	19
Figure 12: Mock cable band attenuation experiment Amplitude vs. time graph	19
Figure 13: Mock cable band attenuation experiment Hit rate vs. Time graph	19
Figure 14: Waveform of a typical corrosion source	20
Figure 15: Waveform from a typical frictional source.....	20
Figure 16: Amplitdue vs. Time for channel 14 on the north cable of AW [Gostautas et al., 2012]	21
Figure 17: Amplitude vs. Date&Time graph from field test experiment	22
Figure 18: Mock-up cable specimen and environmental corrosion chamber; Left: angled view of specimen.....	24
Figure 19: Sensor arrangement in cable cross-section	24
Figure 20: Environmental variable distribution as recorded from the Manhattan Bridge on August 1, 2011	25
Figure 21: Scan measurement chart for suspension bridge suspender rope [Sugahara et al., 2013]	26
Figure 22: Dehumidification system layout for Little Belt Bridge, Denmark. [Bloomstine & Sorenson 2006]	28
Figure 23: Typical dehumidification plant (left) and diagram of active sorption rotor (right). [Bloomstine 2011]	29
Figure 24: Cableguard™ wrapping application. [dsbrown.com]	29
Figure 25: S-shaped wrapping wire and flexible paint corrosion protection systems. [Eguchi et al. 1999]	30

List of Tables

Table 1: Comparison of Average Hit Rate for Experiments with Saline Solution.....	16
Table 2: Percentage of hits from R.45 sensor which passes the filter	20
Table 3: Percentage of hits passing the graphical filter from periods of the AWB shutdown.....	21

1.0 Introduction

The Ohio Department of Transportation is beginning a large rehabilitation project for the 82 year old Anthony Wayne Bridge (AWB) in Toledo, Ohio in 2014. The goal of the rehabilitation is to extend the life of the Anthony Wayne Bridge by at least 50 years. The initial phase of the project includes replacement of the fracture critical trusses supporting the approach spans, redecking the bridge, replacing the sidewalks, fence and railings, and general rehabilitation of the structure. This portion of the project is scheduled to take nineteen months, from spring 2014 through 2015, during which time the bridge will be closed to traffic. In 2016, ODOT will begin work on rehabilitation of the main cables. In preparation for this work, the Department has expressed interest in evaluating monitoring and protection strategies which may extend the life of the AWB. This study was proposed and performed in line with this goal.

Monitoring and maintenance of suspension bridge cables is inherently difficult. Most cable protection strategies utilize a wire or elastomeric wrapping system in order to shield the cable from outside elements. The presence of the wrapping restricts visual inspection and makes it very difficult to predict how the cable is aging. The case study of the Waldo Hancock Bridge is the perfect example of why the development of better monitoring and inspection techniques is so important. In 2002, the 70 year old bridge, laid up with twisted wire strands, was undergoing a cable rehabilitation project. During this project it was discovered that the level of corrosion was much more advanced than originally anticipated, based on previous inspections. In one location corrosion was so severe that an entire strand had already been broken, and surrounding strands were loose, carrying no load [Pure Technologies LTD, 2004]. In order to maintain regular traffic, an emergency installation of secondary cables was designed. They calculated that this procedure increased the factor of safety from 1.8 to 3.2. This case study shows the evident problems which can occur given the infrequent and all too limited inspection practices of today.

The completion of this study provides additional knowledge regarding the latest corrosion monitoring and cable preservation techniques available. In addition, it provides the foundation for potential future monitoring of active corrosion through acoustic emission.

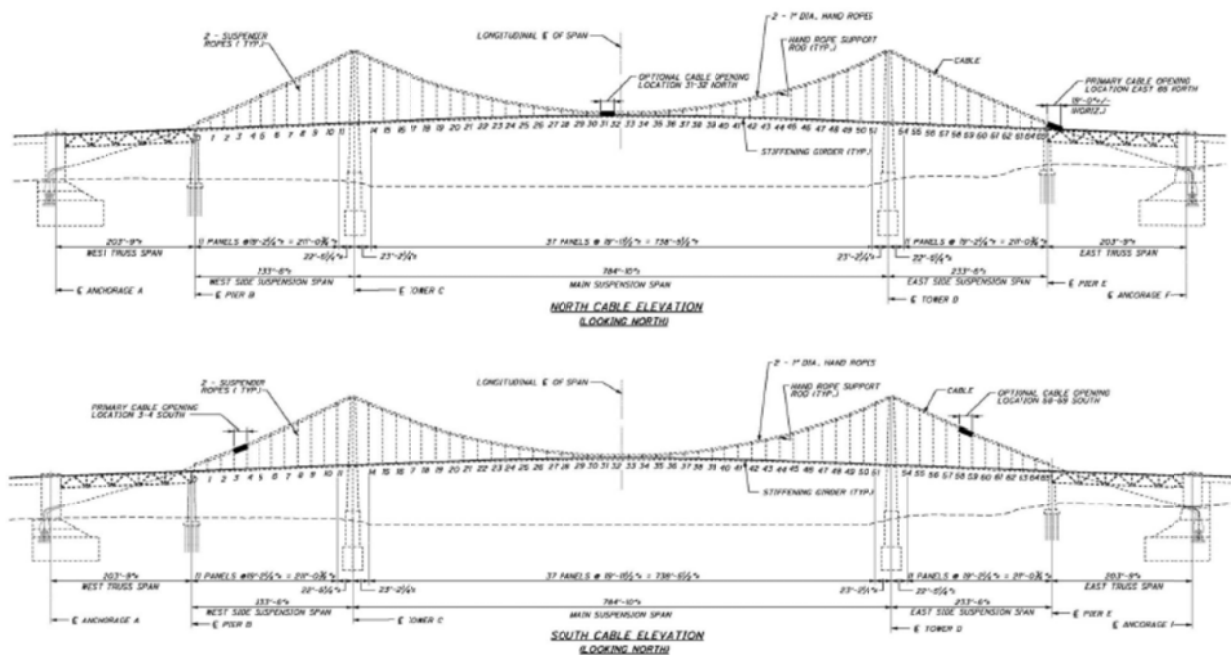


Figure 1: Elevation drawing of the north and south cables on the Anthony Wayne Bridge [2013 Cable Strength Evaluation Report]

1.1 Description of bridge

The AWB is a suspension bridge with a main span of 785 feet and two side spans each of length 233.5 feet. Including the approaches, the full length of the bridge is 3215 feet. The Anthony Wayne Bridge features two 13-5/16 inch diameter, parallel wire main cables, each of which contains 19 strands consisting of 186 No. 6 galvanized steel wires. The current protection system includes a red lead paste, a continuous wire wrap, and an elastomeric wrapping as the exterior protection. Suspender ropes run between the deck and cable bands at intervals of approximately every 20 feet along the suspended spans, creating a total of 118 panels between the north and south cables. The roadway is supported by a stringer and floorbeam system. The bridge carries four lanes of S.R. 2 across the Maumee River, two lanes in each direction, with an average daily traffic of approximately 24,000 vehicles. An elevation of the bridge can be seen on the previous page (figure 1).

1.2 Recent Monitoring & Inspections

Monitoring System

In line with the above mentioned goals, the main cables of the AWB were fitted with an acoustic monitoring system which has been actively listening for wire breaks since July of 2011. The monitoring system includes 15 low frequency sensors spaced at roughly 100 foot intervals along each cable. The sensors on both cables are hard lined into the Sensor Highway II data acquisition system. The data from the acoustic monitoring is stored temporarily and then sent wirelessly over a cell phone connection to a remote location. It is also possible to log into the system via the internet and watch the real time acoustic emission (AE) data. The AE system continuously provides an overview of the health of the entire cable volume. The system has also been used to identify potentially useful locations for internal inspection. To date there have been no wire breaks recorded.

Invasive Inspection

In fall of 2012, ODOT performed an invasive inspection of the AW main cables generally following the NCHRP Report 534 guidelines. A report titled the "2013 Cable Strength Evaluation Report" describes this inspection and was submitted to ODOT in February 2013 by Modjeski and Masters. During this inspection a total of four panels were opened, two per cable. The panels inspected on the north cable include the low point at mid-span and the panel at the far end of the east side span, just before the cable passes through the deck. On the south side the panels inspected were on either side span. The panel on the west side span was only about 1/3 of the way up, while the panel on the east side span was approximately 2/3 the way up the cable. The approximate locations of these windows can be seen in figure 1, on the previous page.

A total of 13 samples were taken during the inspection (three to four at each opening) for testing. The remaining cable strength was estimated utilizing both the Simplified Strength Model and the Brittle Wire Model, which may be conservative depending on the condition of the wires in the bridge. The Limited Ductility Model requires the ultimate strain at failure of each specimen as well as a full stress-strain curve. For unknown reasons, the laboratory testing did not record the ultimate strain at failure, eliminating this model from strength estimating calculations. Due to the relatively low number of samples taken, it is likely wiser to utilize the more conservative Brittle Wire Method.

The resulting, controlling, factor of safety for the cable based on the results from the Brittle Wire Method is 2.41. The strength evaluation report estimated that the factor of safety on the cable will reach the critical point of 2.15 in 2025, just 13 years after the cable inspection.

1.3 Background on AE

The acoustic emission system plays an important role on the AWB and throughout this research. As part of this study, a number of experiments are performed utilizing a mobile acoustic monitoring system. For those unfamiliar, a brief introduction to the technology and related terminology should provide the necessary background to understand the experimental analysis presented in this report.

Acoustic emission describes the elastic transient response, in the form of a wave, which is generated by some sort of deformation or applied stress during a source event. This wave is detected by an acoustic sensor. The sensor is able to detect the deformation in the material as the wave passes, generating a voltage. The voltage is then converted into discernible data through a proper data acquisition system (DAQ). The source, or source event, is the mechanism from which the wave originates. An acoustic event is a source which can be tracked to a physical location. To locate a source along a line the wave must be detected by two or more acoustic sensors. In the case of corrosion monitoring with AE on a bridge cable, the signals are too low to be detected by multiple sensors. Any wave which is only detected by one sensor is known as a hit. In order for a hit to be detected, it must have sufficient strength to pass a user defined threshold. Each hit which is detected by the sensor represents a waveform which in turn can be defined by a number signal features or parameters.

Figure 2 diagrams a sample waveform (or hit) and illustrates the associated parameters. The amplitude of the wave corresponds to the level of voltage produced by the sensor. When converted by the DAQ the amplitude is typically represented in decibels (dB). The threshold is set to the desired amplitude, and will not record any hits which do not meet this level. Rise time measures the time between the first crossing of the threshold and the peak of the wave. Duration is the time between the first and last crossing of the threshold for the same hit. The amount of energy in a signal is defined as the area encompassed by the signal envelope, and is shaded in yellow in figure 2. A count is the number of times a signal crosses the threshold. The characteristics of the signal are related to both the source and material through which the wave passes. Additional signal features, such as average frequency, can be determined using the signal processing software.

In this study, the DAQ is the Mistras Pocket AE and the associated signal processing software is AEwin. AEwin allows the creation of graphical layouts which help the user obtain the desired information from the AE data. Once the data has been collected, users are able to replay the data file through the graphical layouts providing for simplified data analysis.

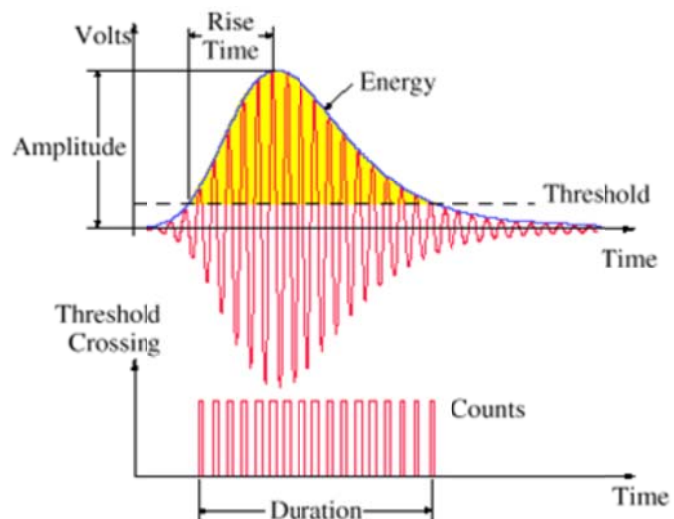


Figure 2: AE waveform features [Gostautas et al., 2012]

2.0 Research Objectives

The overall goal is to lay the groundwork for long term continuous monitoring of the aging of the main suspension cables of the Anthony Wayne Bridge. ODOT has begun this process by installing an acoustic monitoring system on the bridge which is capable of detecting wire breaks. The wire break monitoring can provide insight into cable deterioration throughout the whole volume of cable, but only after a wire has deteriorated enough to break. The ability to detect active corrosion would allow more time for ODOT to plan any potential maintenance required for the cable. Monitoring the most severely corroded sections of the cable would aid in more accurately depicting remaining cable life. There are four objectives that support the overall goal:

- 1) Assess if the installed wire break acoustic monitoring system can be practically used to detect active corrosion. This objective includes assessing the effectiveness of the existing sensor to detect the corrosion signal, the ability to filter the corrosion signals from background noise, and to determine a practical application strategy for use on the AW.
- 2) Determine what sensors, if any, it may be practical and useful to embed in the main cable. Such internal sensors have been tested in both laboratory, at Columbia University, and field settings, the Manhattan Bridge, which monitor the conditions inside the cable. Tests have found that interior conditions are not uniform and that they are capable of fluctuating fairly quickly. There is potential to use the information from the sensors to monitor the corrosion rate at various locations in the cable. In addition, internal sensors may compliment additional technologies such as corrosion monitoring with AE or cable dehumidification.
- 3) Assure that the proposed system for main cable health assessment comprehensively considers the available technologies. The technologies should include both cable monitoring and preservation methods. This study will report on the background of the technology, testing of the technology, results of implementation of the technologies (whenever applicable) and potential for application of the technology to the AWB.
- 4) A preliminary analysis of the cost trade-off for reviewed monitoring and protection strategies should be included.

3.0 General Description of Research

This research supports the on-going effort by ODOT to determine the best available techniques for monitoring and preserving the main suspension cables of the Anthony Wayne Bridge. The project will target corrosion as the primary aging mechanism of the main suspension cables. The research will be performed through two major approaches. The first is hands-on research, as befits a student study, to determine if the current sensors may be used to reliably identify active corrosion. Laboratory experiments were performed to understand and characterize the corrosion of high strength bridge wire and to determine if the acoustic emissions from corrosion can be filtered from other noise sources. Additional tests were performed with the specific purpose of evaluating the potential capacity of the existing sensors to monitor corrosion.

The second involves a comprehensive literature review of state-of-the-art corrosion monitoring and protection strategies for suspension bridge main cables and discussion with leaders in this field. The monitoring technologies reviewed include the potential use of embedded sensors to be installed within the cable as well as the magnetic main flux method for cable inspection. The contacts at Columbia University have advised the researchers on the advantages of internal sensors for suspension bridge cables. It appears that these sensors could serve as a functional indicator of potential corrosion and cable environment, as well as a valuable research tool. The main flux method has been developed by Cable Technologies North America (CTNA), a local subsidiary of Tokyo Rope MFG. CO. The researchers at UT have met with CTNA and established a line of contact between their company and ODOT. The team has also been in contact with personnel from NYC DOT and Columbia University who have experience working with CTNA on testing the MMFM inspection capabilities.

In addition to monitoring, the research is aimed at identifying strategies for the preservation of the main cables. The researchers have performed a literature review and utilized contacts to gain insight into the effectiveness of cable dehumidification. The technology has seen success in Europe and Japan and is beginning to move into the United States. It is the authors understanding that the Department has ruled out cable oiling as a preservation technique, and it is not discussed in this report.

The final task of this project is to provide a synthesis of the reviewed solutions and identify the best practices based on some combination of the aforementioned strategies.

4.0 Research Results & Findings

4.1 Corrosion Monitoring Experiments

4.1.1 Experimental Background

The use of acoustic emission to monitor corrosion has been tested since the 1970's. Between then and now numerous studies have explored the primary and secondary sources of AE of many types of metal and structural components [Pollock, 1986]. Some of the materials tested include stainless steels [Fregonese et al., 2001; Lee et al., 2008; Mazille, Rothea & Tronel, 1995], buried steel pipes [Yuyama & Nishida 2002], aircraft structures (aluminum) [Pollock, 1986], petroleum storage tanks [Kasai et al., 2008] and oil tankers [Wang et al., 2010] among others. As can be seen, the application of acoustic monitoring has been influential in many industries and is among the most promising of non-destructive technologies. The application to cable supported bridges has come naturally as suspension cables and stay cables are some of the most critical yet inaccessible structural members in service today. The initial use of acoustic emission technology for cables came in the form of wire break monitoring, as mentioned by [Elliott, Paulson & Youdan, 2001; Higgins, 2006]. The application of wire break monitoring on the Anthony Wayne further attests to the reputation of the wire break and acoustic monitoring techniques. Wire break monitoring itself is a source related to corrosion, and can be indicative of problem areas. However, the ability to track active corrosion over time will allow owners of large bridges to plan appropriate inspections, repairs and rehabilitation further in advance, which will maximize the efficiency of money spent and the life of the cable. The advance in AE sensing technology and data processing may provide the necessary tools to identify active corrosion and separate it from other noise sources.

4.1.2 Chemistry of Corrosion

In order to hunt for active corrosion it is important to understand the chemistry of corrosion and where the sources of AE originate. Acoustic emission is the elastic wave which propagates through a material as a result of the release of energy from a source event. In the case of corrosion, the source events can originate from the chemical reaction happening at the surface of the metal, or from mechanical processes which happen as a direct result of corrosion. These concepts are illustrated in figure 3, below.

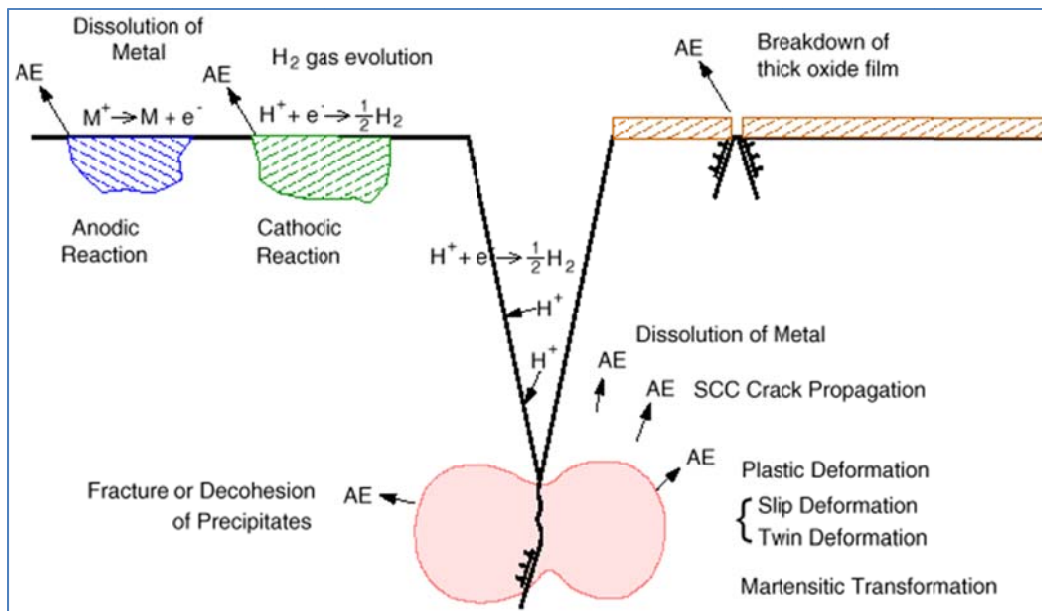


Figure 3: Schematic of A sources during corrosion, SCC and corrosion fatigue processes [Yuyama, 2002]

Corrosion begins when the surface of the metal comes in contact with some corrosive solution and is characterized by two major reactions. These reactions are the oxidation reaction and the reduction reaction, also known as the anodic reaction and cathodic reaction, respectively. During the oxidation reaction, at the anode, the molecules on the surface of the material are oxidized, losing an electron and releasing metal ions into the solution. This is called the dissolution of metal. Simultaneously, the electrons flow through the material to the cathode where they either react to neutralize positive ions, like hydrogen ions, or create negative ions [Roberge, 2006]. When the electrons react with the hydrogen ions this is called hydrogen evolution, as hydrogen gas is formed. Other common reactions at the surface of the cathode are the oxygen reduction reactions. These reactions may differ depending on the acidity of the solution. If the solution is acidic the oxygen tends to react with both hydrogen ions and electrons to yield water molecules. If the solution is more neutral or basic the oxygen will react with the water molecules and electrons to form negatively charged hydroxyl ions. Throughout the process the metal ions will react with the hydroxyl ions to produce various metal oxides which collect on the surface of the material. Depending on the metal, the oxide film may serve to protect the material beneath, such as for aluminum, or simply form and breakdown as the material continues to corrode, as happens in the case of steel. All of these processes are illustrated in figure 3.

The process of corrosion also opens up a pathway for other mechanical sources of deterioration which release AE. Localized corrosion, or pitting corrosion, may cause microcracking along the surface of the material. If the material is under enough tension, the material may develop stress corrosion cracking (SCC) which threatens to eliminate the benefits of plastic deformation in metals, especially high strength steel. The initiation of cracks is the beginning for a number of additional mechanical sources of AE including cyclic loading, which leads to rubbing of crack faces as well as propagating fatigue cracks.

Pollock [1986] lists principal processes of corrosion which includes all of the sources mentioned in the previous two paragraphs. From these it is concluded that the majority of chemical processes, including passage of electric current, dissolution of metal, and film formation do not exhibit a high enough release of energy to be detectable by AE sensors. However, the evolution and rupture of hydrogen gas and the breakdown of the oxide film have both been found to produce AE high enough to detect. A discussion by Yuyama & Kishi [1983] also identifies hydrogen evolution and oxide breakdown as potential sources of AE. These are the primary sources that are targeted during the corrosion studies performed in this study.

4.1.3 Development of the Experimental Program

The objectives of these experiments are to test the ability of acoustic emission sensing to detect active corrosion and to evaluate the practicality of applying the results to monitoring of the main cables of the Anthony Wayne Bridge (AWB). These objectives were explored using two experimental stages. The first was to perform a series of experiments, multiple times, and make observations concerning the characteristics of AE from corroding steel. This stage can be simply referred to as laboratory corrosion cell testing. The second stage of experiments involved three tests which would provide insight into the practicality of utilizing this technology to identify active corrosion on the AWB. The first test was the attenuation experiment in which a corrosion cell was monitored as it was moved along a steel bar further and further away from the AE sensor. The second test includes a field test of the corrosion cell, strapped to a cable band on the AWB near one of the AE sensors. The corrosion signals were recorded by both the pocket AE and the bridge AE system. The third test includes the identification of corrosion signal parameters which can be used to separate corrosion signals from other noise sources on the bridge. The noise sources used in this study include friction and rain. This section will describe the development of testing method, the corrosion cell and the procedures for each test. The following section, "Experimental Results and Discussion", will describe the observations made during the laboratory corrosion cell testing and AWB application testing.

The corrosion cell testing method was determined over a period of months investigating the effects of stress and environment on corrosion. The initial experimental technique would have used a small fixture in which a steel bridge wire would be tensioned while passing it through a trough of corrosive solution. According to a study by [Barton et al., 2000], in which a group of wires were corroded with various preloads, it was found that the level of load did not have a significant effect on ultimate strength of the

wire. During this test it was also found that the ultimate reduction of wire strength was primarily due to loss of section through corrosion, as opposed to stress corrosion cracking or hydrogen embrittlement. These two conclusions show that tension in the wire does not largely impact the corrosion rate or corrosion process of bridge wires. The conclusions drawn from the Barton study were also confirmed by [Cao et al., 2003]. With this in mind, our team, per discussions with Mistras, made the decision to utilize the more simple design of a corrosion cell for these experiments.

There were two critical requirements of the corrosion cell; functionality and mobility. The cell would have to work well in both the laboratory and the field testing stages. The key points of functionality included easy mounting of AE sensors for laboratory testing and effective contact between wires so that the propagation of acoustic waves could transfer efficiently to the sensors. The mobility requirement was simple; it must be easily mountable in a number of test settings, including to an AWB cable band. The resulting design included centering and welding of one half of a 1.5" pipe nipple onto a 4"x4"x1/4" steel plate. Compatible pipe flanges were used to provide additional versatility in mounting for various experiments. Straightened bridge wire was cut to lengths of 1.75" and were wedged together to fill the space of the corrosion cell. The last couple of wires are driven in with a hammer, which creates a compaction force and allows the AE from the wires to transfer to the surrounding wall of the pipe and to the bottom flange, where the sensors are mounted. During testing, corrosion was initiated through filling the cell with a corrosive solution of either tap water or a saline solution. Depending on the test, the cell could either be drained, leaving the wires simply wet, or left full to simulate wires submerged in solution. Due to the slight curve in the small wires, they are not as tightly packed as the parallel wire in a bridge cable. The percent of voids for the cell when filled with wires is about 32%, as opposed to roughly 20% in the case of a typical suspension bridge cable. The cell was tested with and without wires. A picture of the fabricated corrosion cell can be seen in figure 4.



Figure 4: Corrosion cell with wires

The remaining uncertainties included identifying an appropriate length of time to run the test, identifying appropriate settings for data acquisition, and creating a solution to accelerate corrosion. In the end, determining the proper length and data acquisition settings came down to trial and error. Early tests ran for varying lengths of time until it was concluded that longer tests would not provide additional useful information. The primary parameter that was varied during data acquisition was the threshold level. We were initially uncertain what level would be adequate to monitor corrosion. Eventually we settled on 45 dB, which is the same threshold used during the AWB shutdown in October of 2011 [Gostautas et al., 2012]. The solution created to accelerate corrosion was the product of reviewing a number of similar experiments. [Barton et al., 2000] utilized a cyclic fogs solution with up to 5%NaCl by weight and a pH of 3, adjusted with acetic acid, to corrode high strength bridge wire. [Cao et al., 2003] corroded high strength bridge wire as well utilizing a fog solution with 0.05% NaCl, by weight, and a pH of 3 adjusted with hydrochloric acid (HCl). Lastly, [Mazille, Rothea & Tronel, 1995] utilized a solution of 3% NaCl by weight and a pH of 2 to corrode austenitic stainless steel. Based on the results of the experiments, all combinations seemed to be effective in accelerating corrosion. The final solution chosen for this experiments mimicked that from the Mazille study; a 3% saline solution with a pH adjusted to approximately 2 using HCl.

The Pocket AE, a portable two channel acoustic emission acquisition system was used during these experiments. Two resonant sensors were used to capture the AE from the corrosion cell simultaneously. The sensors used include the Mistras R15 α general purpose sensor and the R.45 low frequency sensor. The R15 α is a narrow band sensor with a resonant frequency near 150 kHz meanwhile the R.45 has a resonant frequency of about 22 kHz.

4.1.4 Experimental Results & Discussion

Laboratory Corrosion Cell Testing

The laboratory corrosion cell testing explored a large variety of variables throughout over thirty experiments. Tests were designed to compare the AE during corrosion of galvanized and ungalvanized wire, the use of saline solution vs. tap water solution, corrosion of submerged wires vs. wet wires, and the length of the corrosion period. In addition, each of these experiments was recorded with both the R15 α high frequency sensor and the R.45 low frequency sensor, for comparison. The test set-up can be seen in figure 5, to the right. In general, since the true goal of this research was to apply findings to the Anthony Wayne Bridge, the results presented in this report will primarily compare data obtained by the R.45 sensor; which is the sensor used on the AW. The results of these tests are presented in this section.



Figure 5: Set-up for laboratory corrosion cell testing

To keep track of each test, and the variables that were tested, a naming system was established.

Each test name is composed of four parts

separated by a dash. The first portion identifies which corrosion cell is being used and is designated by 'C1' through 'C5'. The second part identifies the state of the wires used. The options for this included NW (no wires), 'G' (galvanized wires), 'UG' (ungalvanized wires) and 'GUG' (galvanized and ungalvanized wires). The third part in the test name refers to the solution used to corrode the cell and whether the wires were wet or submerged. The options for the third part include 'SS3' (submerged with 3% saline solution), 'SW' (submerged in water), and 'WS3' (wetted with 3% saline solution). The last part identifies the test as the first, second or third of its kind. An example name of an experiment is C4-G-WS3-2. In this test corrosion cell 4, containing galvanized wires, is corroded by wetting the wires with the 3% saline solution (with pH of 2) and it is the second time the test was performed.

The testing was performed in two phases in order to attempt to determine the amount of AE generated from the corrosion of the wires vs. the corrosion of the cell without wires. During the first phase the exact same tests were run sans wires. The surface area open to corrosion increases from 9.08 in² to roughly 45.98 in², an increase of about 500%. The increase in average hit rate (total hits in the experiment over the total time) was about 400 to 800% for experiments using galvanized wire, showing the participation of the wires in the recorded AE. However, the experiments which utilized ungalvanized wires did not show an increase in the average hit rate. Prior to evaluating additional data, this suggests the galvanized wire (with zinc being oxidized, as opposed to steel) produces signals that are easier to detect by the AE technique.

Comparison of AE from Galvanized Wires vs. Ungalvanized Wires

In general, it was found that galvanized wires produced a higher amount of AE than the corresponding experiments using ungalvanized wire. Table 1 shows the comparison of several experiments and the associated average hit rate. The two experiments with submerged wires were the same, apart from utilizing galvanized and ungalvanized wires. The same is true of the experiments with wetted wires. Each test was performed three times, so the hit rate in the table is the average of the three tests.

Table 1: Comparison of Average Hit Rate for Experiments with Saline Solution

Description of Experiment	Average Hit Rate (hits/hour)
C2-G-SS3-1:3 (submerged galvanized wires)	1071.8
C3-UG-SS3-1:3 (submerged ungalvanized wires)	149
C4-G-WS3-1:3 (wetted galvanized wires)	198
C5-UG-WS3-1:3 (wetted ungalvanized wires)	66.6

As table 1 shows, the AE hit rate during the test with submerged galvanized wires is over seven times more than that of the same test using ungalvanized wires. In comparing the experiments with wetted corrosion cells, the cell with galvanized wire had nearly three times the hit rate of its ungalvanized counterpart.

Another difference between the galvanized and ungalvanized experiments is the shape of their curves. The experiments with galvanized wires show a near constant curve with less variability at the beginning of the test. In contrast, the experiments with ungalvanized wires show a bi-linear curve including a steep portion during the first few thousand seconds of the test, followed by a plateau with a drastically reduced hit rate. The plateau generally remained at a constant hit rate until the completion of the test. While the exact reason for the bilinear curve is unknown, it is possible that it relates to the rate of diffusion of hydrogen ions and dissolved oxygen throughout the solution. This would justify a high initial rate, followed by a slower, stabilized period. However, this description can also be used to describe the shape of the hit vs. time curve during the corrosion of an empty cell with no wires. Despite the formation of obvious corrosion debris, there does not seem to have been a high additional participation of the ungalvanized wires in the data recorded by the AE sensors.

Figures 6 and 7 show the shapes of the hit vs. time curves for C3-NW-SS3-2 and C3-UG-SS3-2, respectively. Figure 8 provides the same graph for an experiment with galvanized wires, C2-G-SS3-2, for comparison.

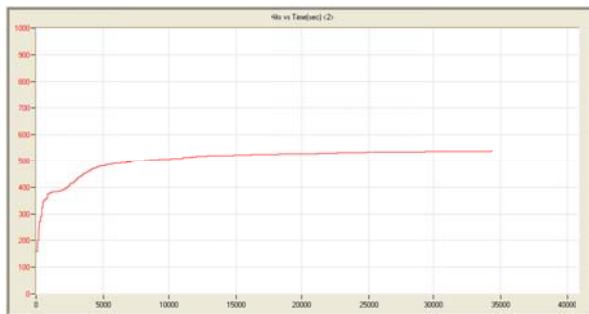


Figure 6: Hits vs. time for C3-NW-SS3-2

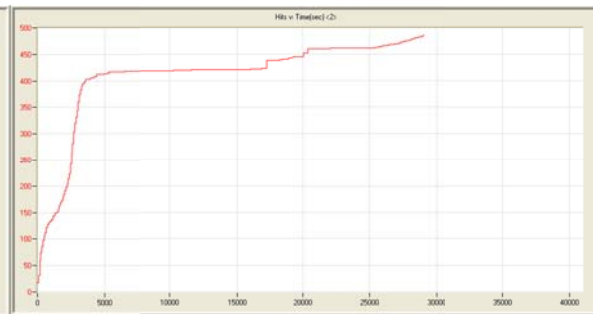


Figure 7: Hits vs. time for C3-UG-SS3-2

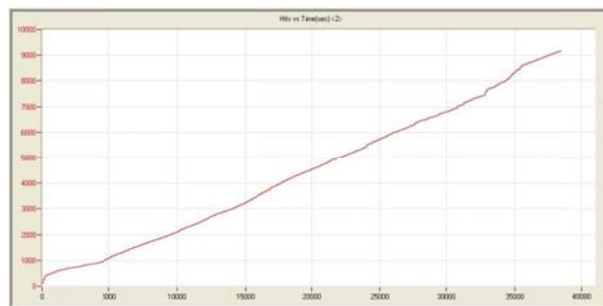


Figure 8: Hits vs. Time for C2-G-SS3-2

Comparison of Wetted Wires Corrosion vs. Submerged Wire Corrosion

Reviewing previous studies, it was identified that a salt fog was highly effective for accelerating corrosion [Barton et al., 2000; Cao et al., 2003]. Although we were unable to utilize a fog, we realized that wires inside a cable may be wet at times, or completely submerged by water, depending on the rate of nearby infiltration into the cable. For this reason we decided to test the potential difference in AE generated by the settings. Table 1, in the previous section, can be used to compare the experiments with submerged wires to those with wetted wires. Tests with submerged and galvanized wires produced a hit rate over five times greater than the tests with wetted and galvanized wires. Looking at the same comparison for tests with ungalvanized wires, it can be seen that the hit rate is twice as large for submerged wires vs. galvanized wires. In addition, it can be seen visually that there was much more corrosion during the tests with submerged wires (C1, C2, C3). This is illustrated in figure 9. It is clear that in the case of AE, corrosion of submerged wires is much more readily detected.



Figure 6: Visual of cumulative corrosion for each cell after completion of laboratory testing

Comparison of the Use of Saline Solution vs. Tap Water

Corrosion cell C1 was used as a control cell to which corrosion generated in other cells could be compared. In order to do this the corrosive solution used in C1 was tap water. In addition, C1 was used during attenuation experiment and on bridge testing. In an attempt to accurately simulate the wires corroded in the cable band, the cell included both galvanized and ungalvanized (GUG) wires. Like the Anthony Wayne cables, the majority of the wires used were galvanized. However, a number of the exterior wires were replaced with ungalvanized wire which represents stage four corrosion on the exterior of the bundle.

Although the corrosion cells which utilized the saline solution showed significantly more visible corrosion, the AE generated by C1, filled with tap water, produced near equal hit rates. In fact, the test which generated the highest hit rate was C1-GUG-SW-3, achieving an extraordinarily high hit rate of over 25,000 hits per hour. The average of the other tests of C1 is 1079 hits per hour, which is very similar to the 1071.8 hits per hour recorded while using the saline solution in C2. Why this test was so prolific is not immediately identifiable. There was not much difference in corrosion characteristics between the control cell and those which contained the saline solution.

Comparison of Variable Lengths of Corrosion Periods

The lengths of experiments during these tests ranged from about 6 minutes to approximately two days. The reason behind varying the length of the tests is to determine whether or not the corrosion rate might change as time passes. Although these are relatively short periods of time in the world of corrosion, it was found that, in general, once corrosion has stabilized, the hit rate will remain constant so long as the environment remains constant. That is to say the hit rate will only begin to decrease when the solution has significantly evaporated. Longer tests would need to be performed to make this conclusion for certain.

There was one test, however, that did not exhibit this behavior. The hits vs. time curve for test C3-UG-SS3-1 can be seen in figure 10. As can be seen from the graph, there is very little AE activity for the first 40,000 seconds of the test. At approximately 43,000 seconds the hit rate surges and reaches about 1300 hits per hour, for a period of nearly two and half hours until quickly returning to a rate that is close to zero. This test could indicate that corrosion of ungalvanized steel wire has some sort of cyclic tendency, although it was not apparent in any of the other equivalently long tests. It should also be noted that the increased hit rate actually included more hits on the high frequency sensor than the low frequency sensors, which is abnormal based on the other experiments. It seems the surge in AE may have been produced by a source which generates signals with a higher than normal average frequency. As mentioned previously, additional experiments with longer testing periods could provide clarification as to whether or not this test was some sort of anomaly or error.

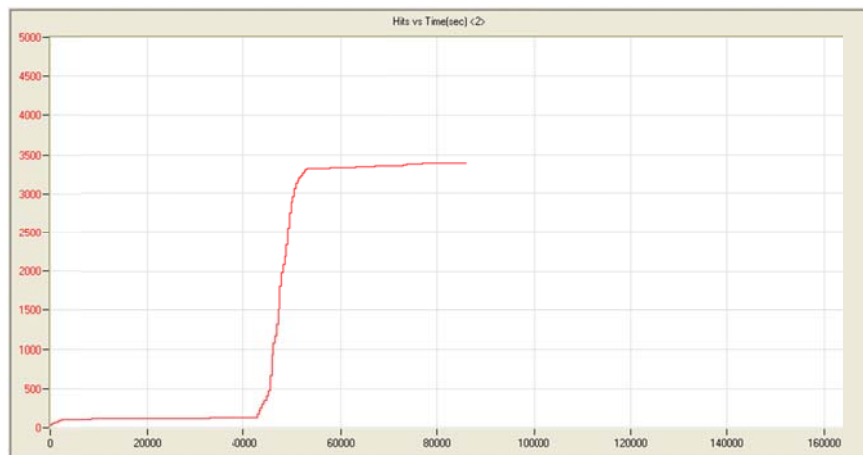


Figure 7: Hits vs. time for C3-UG-SS3-1

It was also found that the test should be run for at least 2 hours prior to obtaining any reliable and stable hit rate from corrosion. During many experiments, the hit rate would initially begin at a high level, but level off between 2000 and 5000 seconds. If the experiment was too short, it would yield an unrealistically high corrosion rate.

General Comparison of High Frequency & Low Frequency Sensors

The use of the R15 α , high frequency sensor, in combination with the R.45, low frequency sensor provides an additional angle at which to view and evaluate the data. If AE sources produce signals at significantly different average frequencies it would be easily detected by watching the data from both sensors. During these experiments, the average frequencies of the majority of hits tended to favor the low frequency sensor. The average number of hits per experiment recorded by the R.45 sensor is 2480, as compared to 874 for R15 α . The majority of these hits occurred somewhere in the range of 5 to 50 kHz. As the R.45 sensor is currently what is mounted on the AWB, the sensitivity the sensor seems to have for low level corrosion signals is encouraging.

Anthony Wayne Bridge Application Testing

Mock Cable Band Attenuation Experiment

It is well known that the corrosion process produces very low level acoustic emission. It was understood going into this project that at best we would only be able to hear corrosion within a few feet of the sensor, which is mounted on a cable band. The objective of this experiment was to reasonably approximate the ability of sensors to record acoustic emission along anypoint near the cable band. To simulate this, a corrosion cell was clamped in place at 6" intervals along a 72"x1-3/4"x3/4" steel bar. The corrosion cell, C1, was filled with tap water a few hours prior and monitored in order to ensure a stabilized hit rate prior to starting the experiment. Once the experiment was started, the corrosion cell was moved 6" further away from the sensor at time intervals of approximately 30 minutes. Time marks can be seen in figures 12 and 13 which indicate when the data collection was paused for moving the cell. The figure on the left shows amplitude vs. time while the figure on the right shows the cumulative hit vs. time curve. If there were attenuation, the left graph would show a gradual reduction in peak amplitudes while the right figure would show a changing hit rate. Both of the graphs indicate that there is no attenuation seen during this experiment. This test shows that if a corrosion source has near direct contact with the cable band, then it is probable that it can be detected by the acoustic emission sensor given a proper threshold.

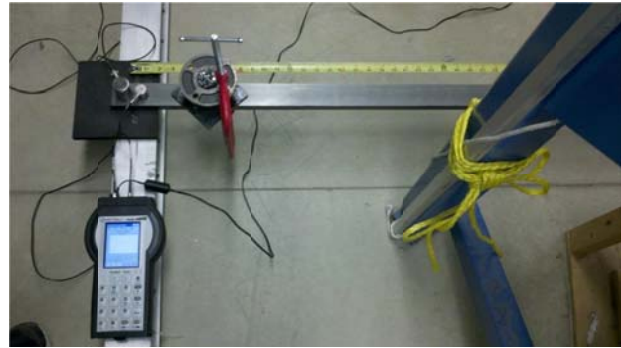


Figure 8: Set-up for mock cable band attenuation experiment

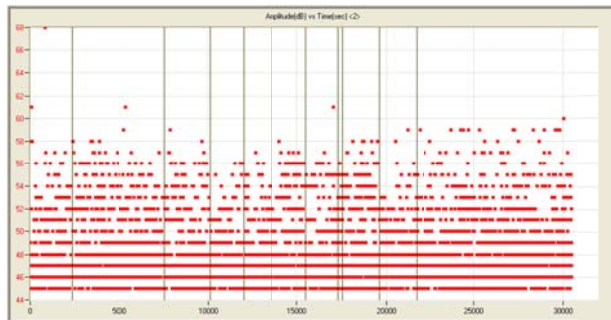


Figure 102: Mock cable band attenuation experiment Amplitude vs. time graph

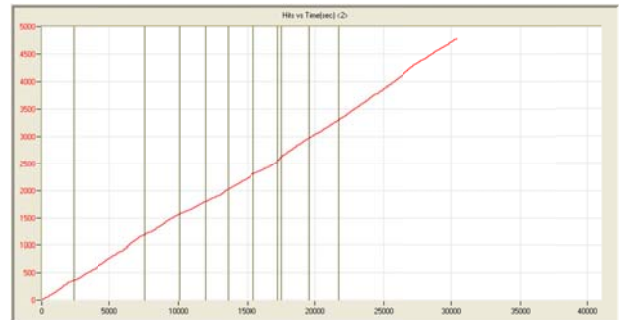


Figure 93: Mock cable band attenuation experiment Hit rate vs. Time graph

Corrosion Signal Characteristics Filter

Throughout the testing it became clear that the corrosion signals were significantly different from the typical frictional signals. This was first apparent after extensive examination of the waveforms generated from the corrosion cell experiments. A corrosion waveform, represented by figure 14, most often has a well-defined peak, near the beginning of the signal, with a gradual exponential decay along the signal envelope. In order to make a direct comparison, a friction experiment as performed to generate real frictional data to be examined. To closely approximate the friction of rubbing wires, an unused corrosion cell was converted into a miniature cable band. A longer wire was thread through the center of the cell while smaller wires were packed into the cell around it. With the sensors mounted, the longer wire was

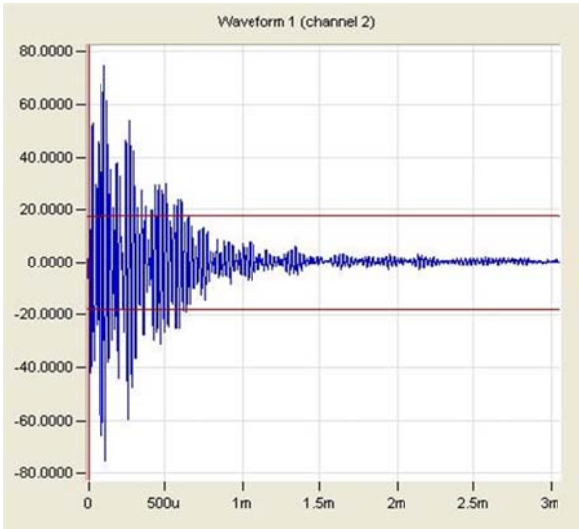


Figure 11: Waveform of a typical corrosion source

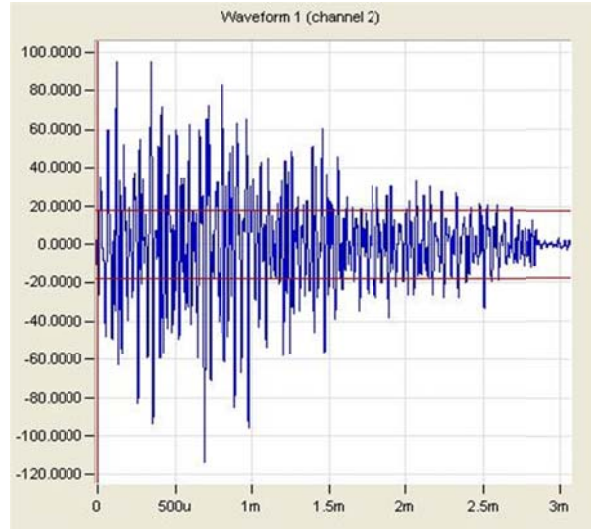


Figure 12: Waveform from a typical frictional source

slowly displaced by small amounts, rubbing against the surrounding wires. The waveform presented in figure 15 is highly representative of the typical friction signal from that test. Given the waveforms, one could begin to separate corrosion signals from friction signals. Unfortunately, due to limited space during data acquisition, the acoustic monitoring system on the AWB is limited to only records select waveforms.

Since it is impractical to record the waveforms from every hit on the bridge, especially at a lowered threshold, it was then required to identify the characteristics of the typical waveform which defines corrosion. Examination of the data showed that most corrosion signals fell within certain ranges of duration, average frequency and rise time. The upper and lower limits to these ranges were chosen by analysis of the Duration vs. Time, Duration vs. Average Frequency and Rise Time vs. Amplitude graphs. The following ranges were identified: 0 to 800 μ s duration, 10 to 200 kHz average frequency, and 0 to 400 μ s rise time. By applying these ranges as graphical filters, we were able to determine the corresponding percentage of hits which passed through all three categories. Table 2 shows the comparison of the percentage of hits recorded by the low frequency sensor which pass through the filter. The table shows that the percent passing changes depending on the conditions of the corrosion; however, C1, the cell that most closely represents the likely conditions in the cable, had the highest rate of passing.

Table 2: Percentage of hits from R.45 sensor which passes the filter

Description of Experiment	Percentage of Hits Passing Filter
C1-GUG-SW-1:2 (Submerged galvanized/ungalvanized wires)	85%
C2-G-SS3-1:3 (submerged galvanized wires)	78%
C3-UG-SS3-1:3 (submerged ungalvanized wires)	72%
C4-G-WS3-1:3 (wetted galvanized wires)	72%
C5-UG-WS3-1:3 (wetted ungalvanized wires)	68%

The graphical filter was also applied to the data from the friction tests in order to determine how well the filter could isolate corrosion. The percentage of frictional hits passing the filter was determined to be 21.5%. Looking at the data more closely, it was found that the frictional hits which passed the filter still maintained the traditional shape of a frictional waveform. It was also found that these hits typically had lower amplitudes; many with only one peak passing the threshold (in figures 14 and 15, the threshold is represented by the two red lines, positive and negative). Since the parameters of duration and rise time

are recorded relative to the threshold, this leads to a number of signals which have a duration and rise time of nearly zero. In reality, the single crossing peak is just the tip of the iceberg, and does not give a true representation of the characteristics of the entire hit. One way to account for this is to establish both a front end threshold and a graphical filter on amplitude. Setting the graphical filter 5 or so dB above the front end threshold allows the hits above the graphical amplitude filter to be evaluated by durations and rise times which consider a larger portion of the full signal. Using this technique, the amount of friction which passed the graphical filter from the frictional tests was reduced to roughly 5%. The downside to using the graphical amplitude filter is the decrease in the total amount of hits which are able to be recorded.

The established graphical filters were also used to evaluate some of the AWB Shutdown Data which was originally discussed in [Gostautas et al., 2012]. The hope was to use the graphical filter to confirm the areas of potential corrosion identified in the report. The figure below is taken from the [Gostautas et al., 2012] SMT conference paper.

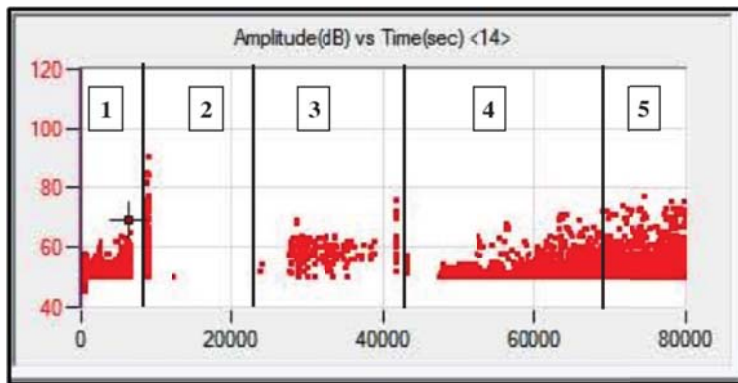


Figure 13: Amplitude vs. Time for channel 14 on the north cable of AW [Gostautas et al., 2012]

Figure 16 shows the Amplitude vs. Time of hits recorded by channel 14 during the shutdown. The graph is broken up into 5 periods. The first period shows normal traffic loading on the bridge. The second period is the time just after the bridge closure, and is relatively quiet. Period three is characterized by an increase in wind loading on the bridge, potentially causing frictional noise. Period four included reduced wind gusts and the beginning of increased relative humidity. Period 5 consisted of a rain event and increasing relative humidity. The data from various channels from both the north and south cable was replayed utilizing the corrosion characteristics filter to analyze the 3rd, 4th and 5th periods during the shutdown. The resulting percent passing the filter during each period, for each channel, is presented in table 3.

Table 3: Percentage of hits passing the graphical filter from periods of the AWB shutdown

Channel	Percent Passing from Period 3	Percent Passing from Period 4	Percent Passing from Period 5
Channel 8 North	5.4%	6.6%	23%
Channel 14 North	74.2%	2.3%	10.1%
Channel 7 South	19.4%	N/A	19.8%
Channel 8 South	2.65	3.7%	18.3%
Channel 11 South	71.3%	58.8%	36.3%
Channel 12 South	20.3%	18.75%	21.3%

Overall the results from studying the shutdown data are inconclusive. It is likely that the majority of the hits during the wind and rain periods can be considered noise, due to the friction or rain. If that is the case, then the filter was able to remove almost 80% of undesired hits on average, although the actual

percentages are scattered. This is similar to the rejection rate of the frictional data generated in the lab mentioned previously. In addition, none of the channels, apart from Channel 11 South, seem to support the potential for active corrosion during period three. Based on the data, it is difficult to evaluate the performance of the filter. Additional testing and refinement would be needed to increase reliability of a corrosion isolating filter.

Field Testing of Corrosion Cell

The goal of this final test was to mount a corrosion cell onto a cable band on the AW and use the existing sensors to detect the active corrosion from the cell. The original plan was to attach the corrosion cell to the cable band and monitor the acoustic emission with both the existing system and the portable Pocket AE system.

In order to run this test, the researchers received access to the log-in information for the remote monitoring of the AW SHII data acquisition system, as well as access to the data storage in order to retrieve data from the time of the test. This test was attempted three times, the first two of which never got off the ground due to weather, and technical difficulties. During the most recent attempt, the team was required to adapt from originally anticipated methods of mounting the corrosion cell and the second AE sensor. During the test, an unexpectedly large amount of wind was experienced, which resulted in a large amount of noise detected by the sensor connected to the Pocket AE. It is suspected that due to the angle and method with which the sensor was mounted (essentially taped onto the side of the cable band), the full range and sensitivity of the sensor was not utilized. The data from the Pocket AE did not identify active corrosion.

The data from the sensor on the center low point, on the south cable, was also examined. The resulting Amplitude vs. Date and Time graph is shown below (figure 17). The center punches used to identify the time in which we were at the cable can be seen at the top middle of the top graph, within the blue circle. The graph shows periodic sets of hits likely caused by a strong gust of wind or large truck. In most cases the graphical filter was able to eliminate the majority of that noise. There is no indication that corrosion was detected from the attached corrosion cell.

This data does however represents the typical noise level of channel 8 between 4:30 AM and 6:30 AM on Sunday morning. Based on the abundant amount of corrosion AE generated in some of the tests, given the right conditions, it would definitely be possible to detect corrosion at that level and consistency.

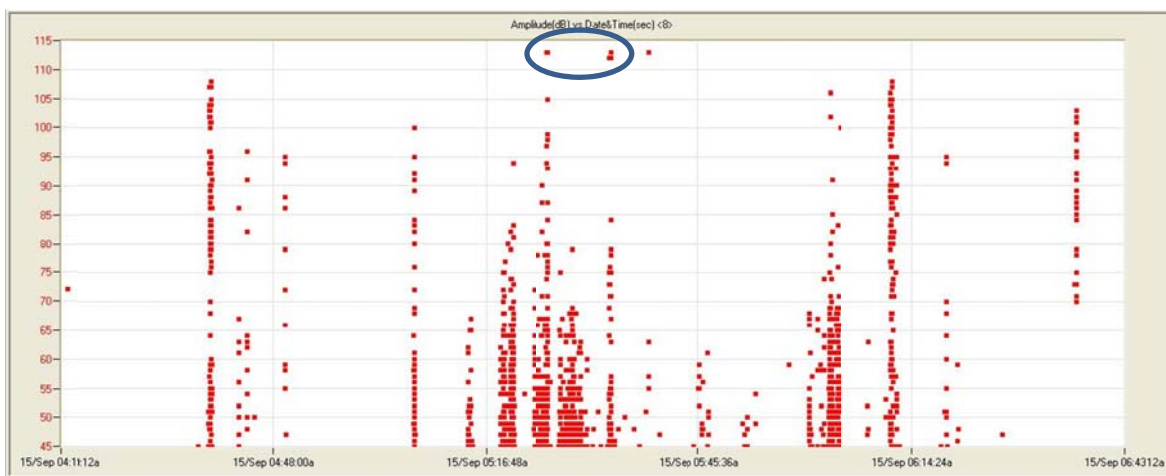


Figure 14: Amplitude vs. Date&Time graph from field test experiment

4.2 Findings from Review of Monitoring and Preservation Technologies

4.2.1 Internal Sensor Technology

Overview

While suspension bridges have allowed man to span tremendous distances, they have also troubled engineers and owners the world over. The main cables, the key structural element of these iconic structures, are fracture critical and therefore must be maintained to have a high level of reliability. The NCHRP Report 534 recommends remedial action when the cable has deteriorated such that the estimated factor of safety for the cable reaches 2.15. It is known that corrosion of the high-strength steel wires is the primary cause for the aging and deterioration of suspension bridge cables [Sloane et al., 2012]. To protect against corrosion engineers have developed protection systems including corrosion inhibiting paste, painting, wire wrapping and elastomeric wrapping. However; these solutions represent a double edged sword. The wrapping, which is intended to keep water out, also keeps water enclosed once it finds a way in. It also prevents maintenance personnel from completing a relatively simple visual inspection as can be done with most other structural components. Internal sensor technology can provide a solution to both of these issues and will bring the bridges of yesteryear into the era of smart structures. This is accomplished through the installation of a group of sensors throughout the cable cross-section. These sensors then return information on including the temperature, relative humidity and corrosion rate at that section of cable. Temperature and relative humidity are environmental conditions which have a correlation to general corrosion [Sloane et al., 2012].

The information on internal sensors collected and presented in this report is based on the results of a 5 year research program at Columbia University and sponsored by the FHWA [Khazem, Serzan & Betti, 2012]. The Columbia study included testing on direct and indirect sensing technologies in the laboratory, using a full-sized mock suspension bridge cable, and in the field. The internal sensor package is an indirect sensing technology and was researched thoroughly. A number of combinations of sensors were tested to determine the most applicable for suspension bridge cables. Only those considered most successful will be discussed in this report. This section will include discussions of the sensor technology, the results of laboratory and field testing, sensor package installation and maintenance, and general cost requirements.

Sensor Description

In selecting the proper sensors, the researchers at Columbia identified the following parameters to measure effectiveness: size, accuracy, durability, resistance to compaction forces, environmental durability and sensitivity to environmental variables [Sloane et al., 2012]. The optimal sensors identified after the experimental testing were the Precon HS2000V and Analatom Linear Polarization Resistance (LPR) sensor.

The Precon HS2000V provides a measurement of temperature and relative humidity. The sensor is accurate to 2% within the environmental operating ranges of 32° to 158°F and 0 to 100% relative humidity. The sensor will continue to provide output for temperature in the range of -22° to 212°F. The output is ratiometric and varies with the output voltage from zero to the level of supply voltage. Additional benefits of the sensor include built in temperature compensation, factory calibration, easy field replaceability (relatively speaking) and good stability [PreconUSA.com].

The Analatom LPR sensor directly measures the corrosion rate of a particular metal in a corrosive environment. The environmental operating temperature for this sensor is -40° to 185°F. The sensor can accurately detect corrosion rate between 0.0001 and 10 mm/year.

Laboratory and Field Testing

The direct and indirect sensing technologies were tested utilizing a full scale mock-up suspension bridge cable. The specimen was designed to simulate one panel length of a large suspension bridge main cable with galvanized parallel wire strands. The cable was comprised of 9,271 wires making up 73

hexagonally shaped strands. The majority of the strands were cut to a length of 20 ft, which approximates the distance between two cable bands. However 7 strands were cut to 35 ft and were tensioned to approximate a load slightly higher than typical service load conditions. The load in the cable was carried by a large reaction frame which surrounds the specimen. The compacted diameter of this cable was 20 inches [Sloane et al., 2012]. Figure 18, left, shows an angled view of the cable mock-up.



Figure 15: Mock-up cable specimen and environmental corrosion chamber; Left: angled view of specimen [Khazem, Serzan & Betti, 2012] & Right: heating phase of cyclic environmental conditions [Sloane et al., 2012]

In addition, an environmental simulation chamber was constructed around the cable. This allowed the cable specimen to be exposed to variable weathering through cyclic combinations of rain, heat, air conditioning and ambient conditions. Heating was provided by heat lamps which were installed at the top of the chamber and air condition and ventilation units were used to level temperature and fluctuate relative humidity. Moisture was introduced via perforated PVC pipes which ran along the top of the chamber and simulated rain. An aluminum foil tape was used as a wrapping system to prevent direct contact between the cable and the environmental conditions [Sloane et al., 2012].

The arrangement of the sensors within the laboratory cable can be seen in figure 19, to the right. Included in this diagram are the locations of the embedded HS2000V (17) and LPR (8) sensors throughout the cable cross-section. Sensors are placed along three diagonals of the cable area, separated by 60°. The HS2000V sensors are denoted with a “T” while the LPR sensors are denoted with “LP”. [Sloane et al., 2012] desired to distribute LPR sensors throughout the bottom of the cable, but laboratory construction operations prevented this.

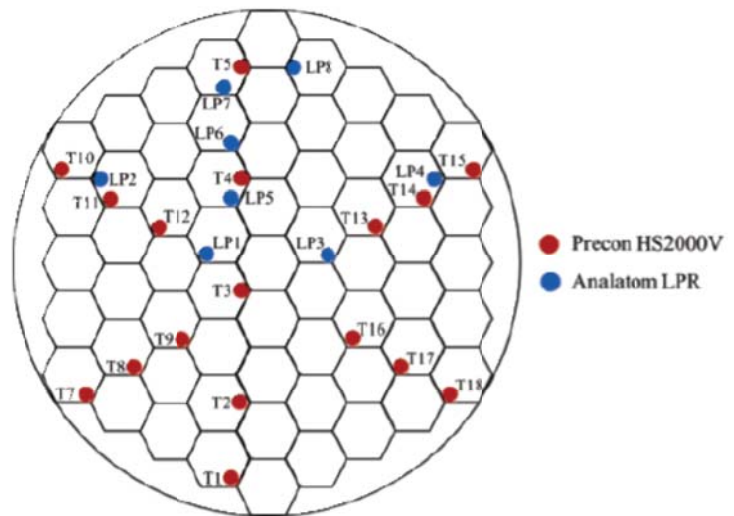


Figure 16: Sensor arrangement in cable cross-section [Sloane et al., 2012]

Each sensor was protected from crushing by small stainless steel tubes which were inserted before and after the sensor within the bundle. The small tubes were 1 inch long and covered with a heat shrinking, moisture resistant coating. The sensors were hard-wired and connected to the Sensor Highway II data acquisition system. The cable was then closed, compacted, and resealed for testing.

The results of the tests identified dynamic environmental conditions within the cable both in the lab and during the field test. As expected, it was found that temperature variations were highest in the outer

layer of wires at the top half of the cable. Although temperature change occurred everywhere, the rate of change was most steady at the center of the cable. Results also confirm the findings from a previous study which concluded that the lower levels of relative humidity can be found in the upper portion of the cable, while higher levels of relative humidity would be found in the sides and lower portion of the cable. In addition, the laboratory data identifies, as expected, an inversed relationship between temperature and relative humidity throughout the cross-section [Sloane et al., 2012].

The corrosion sensors were found to have a strong correlation with local cyclic changes in temperature. This local relationship was not true of relative humidity as it did not show strong cyclic patterns; however, the general relative humidity values did prove to be strong indicators of corrosion based on the data recorded by the LPR corrosion rate sensors.

The field testing was performed in 2011 by installing sensors at one location on the Manhattan Bridge in New York City. The system has been used to record data throughout a number of periods covering multiple days. Figure 20 shows the distributions of temperature (a) and relative humidity (b) throughout the cable cross-section on August 1st, 2011. The embedded sensors proved to be functional and accurate based on the external conditions at the times of data collection, and seem to confirm parameter trends and relationships as seen in the laboratory. The location of minimum temperature corresponds to that of maximum relative humidity experienced that day, verifying the inverse relationship between the two parameters, as expected.

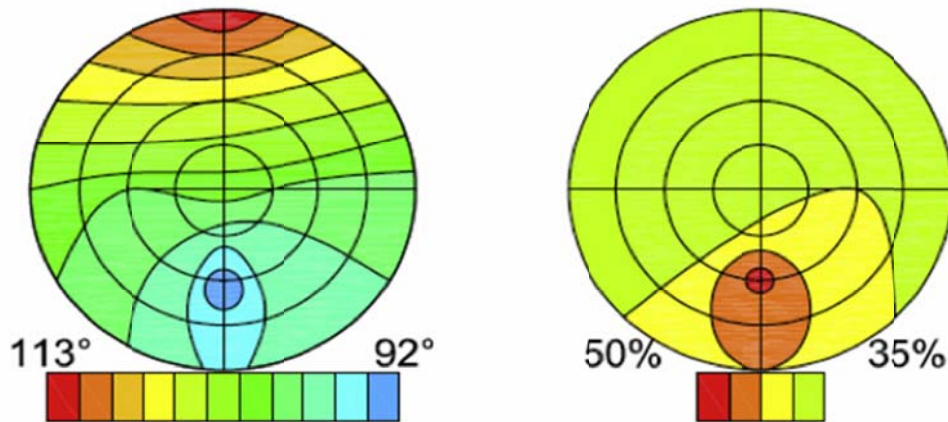


Figure 17: Environmental variable distribution as recorded from the Manhattan Bridge on August 1, 2011
(a) temperature (b) humidity [Sloane et al., 2012]

General Cost Requirements

During the field testing of embedded sensors on the Manhattan Bridge, sensors were placed along the vertical and horizontal axis of the cable cross-section. A total of nine HS2000V and 4 LPR sensors were used. The unit cost of one Precon HS2000V RH & Temperature sensor is \$33.86. Considering the nine sensors, the total cost for the Precon sensor's is \$304.74 per location. The cost of the Analatom LPR sensor is \$182.85 per sensor. The total cost of internal sensor hardware, per location, would be approximately \$1036.14. This does not included any specialty cables, software or other hardware upgrades that would be required for sensor installation and function. It should also be noted, that if implementation should occur, a minimum of two locations would be suggested as a practical minimum.

4.2.2 Magnetic Main Flux Method

Overview

Cable Technologies North America, Inc. (CTNA), a subsidiary to Tokyo Rope MFG. CO. out of Japan, has developed a non-destructive technique for evaluating the condition of structurally critical steel strands or cable with incredible accuracy. The technique is called the Magnetic Main Flux Method (MMFM) and is specifically designed for bridge elements including; stay cables, suspension bridge main cables, suspender ropes and external tendons. The information found in this section is predominantly from a technical paper by [Sugahara et al., 2012] which was submitted to the 2012 SMT Conference in New York. MMFM utilizes the concepts of magnetization to determine the magnitude of deterioration throughout the lengths of cables and strands.

The process of MMFM combines two established measuring options. The first is a scan measurement which was proposed by Weishchdel et al. in 1985. Use of this measurement technique provides only relative change in area along the axial direction of the specimen. The second method, point measurement, was developed by CTNA and utilized alongside scan measurement in order to determine exactly how much material is there. In point measurement, the magnetizer fluctuates the magnetic field at a single point of interest creating magnetic hysteresis loops. Using this data it is possible to produce a quantifiable amount of cross sectional area at that point. The ability to determine cross-sectional area is based on the principle which states that at full saturation, the magnetic flux flowing through a material is proportional to the cross-sectional area of that material. The measuring unit is able to record the magnetic flux along the length of cable, during scan measurement, and determine the area of steel at each location by relating it to a point measurement. The ability to scan the entire depth of cable at each point allows the inspector to identify corrosion on the interior of a strand or cable that cannot be seen from the outside.

The entire system is made up of three units: the magnetizing unit, the measuring unit and the computing unit. The magnetizing unit is comprised of the magnetizer, the electrical cable, a direct current supply, and a polarity switch. The measuring unit includes the search coil, flux meter, hall sensor and a gauss meter. The computing unit simply requires a laptop and data reader in order to log and analyze data.

Laboratory and Field Tests

A number of laboratory and field tests were performed to verify the performance level of MMFM. The tests with relevance to the AW include inspections on suspender ropes and the main cable. Figure 21 shows good agreement between field and laboratory testing of suspension bridge suspender ropes. The region encompassed by the dashed circle in figure 21 represents an area where there was no deterioration outwardly visibly. Upon further investigation, significant corrosion was found on the interior of the strand. The ability to detect deterioration without external indications is one of the major advantages of this technology.

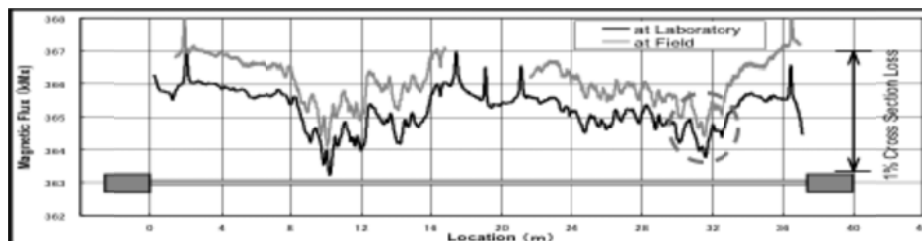


Figure 18: Scan measurement chart for suspension bridge suspender rope [Sugahara et al., 2013]

Additional experiments were performed using the mock suspension bridge cable at Columbia University, and a field experiment on the Manhattan Bridge. The experiment using the mock cable at Columbia involved the placement of additional wires onto the cable to test the sensitivity and accuracy of MMFM.

The system was able to detect variations in cross-sectional area the cable from the addition of steel ranging from 15 to 45 wires. The Columbia cable is 20 inches in diameter and 45 wires makes up approximately 0.05% of the total cross-sectional area. After the encouraging tests in the laboratory, the system was tested on one panel of the Manhattan Bridge. Speaking with a representative from the NYC DOT, they found the results of the field test to be somewhat questionable. MMFM is capable of detecting loss of cross-sectional area due to corrosion. There is reason to believe, however, that the failure mode of wires would also determine the effectiveness of this technology in examining aged suspension bridge cables. Wire breaks in the cable will only be detected if the break was a result of significant loss of section. If the wires are breaking due to a brittle failure mode, such as hydrogen embrittlement, there would not be enough loss of section for MMFM to make that judgment. It appears that prior to utilizing a technology such as MMFM, it should be determined that the wires in the bundle, on the majority, still behave in a ductile manner.

Cost Estimate

In August, representatives from CTNA traveled to the University of Toledo to meet with the researchers and ODOT representatives. CTNA performed a demonstration of the MMFM technology using their system and a corroded strand wrapped in cellophane. At the conclusion of the meeting, ODOT asked if CTNA might generate a quote for various levels of magnetic flux inspection for the AW Bridge. A summary of those cost estimates is represented here and the full cost estimates can be found in the Appendix.

A total of eight options were generated by CTNA for application to the Anthony Wayne Bridge main cables. The options are as follows:

- OPTION 1: Test 4 panels with 1 magnetizer \$179,498
- OPTION 2: Test 118 panels with 2 magnetizers \$913,763
- OPTION 3: Test 12 panels with 1 magnetizer \$245,670
- OPTION 4: Test 12 panels with 2 magnetizers \$304,828
- OPTION 5: Test 4 panels and 4 under cables with 1 magnetizer \$243,582
- OPTION 6: Test 118 panels and 4 under cables with 2 magnetizers \$980,952
- OPTION 7: Test 12 panels and 4 under cables with 1 magnetizer \$312,193
- OPTION 8: Test 12 panels and 4 under cables with 2 magnetizers \$363,018

The cost shown represents only that allocated to the inspection fee as well as to the use of equipment and personnel from CTNA. The engineer and supervisor from CTNA will require assistance from an experienced contractor to facilitate the cable inspection. This relationship would be similar to that between Modjeski & Masters and Piasecki Steel during the November 2012 invasive inspection. The additional cost of the contractor's services is not included. It also does not include the cost of cable band removal, if desired. The removal of bands would not increase the cost of the inspection, but reduce it.

Additional clarification on items from the quotes and inspection procedure is useful to fully understand what the inspection involves. The following sentences provide explanation or background for certain terms from the quote and inspection procedure. 1) The use of 2 magnetizers compared to 1 for the potential 12 panel inspection options is simply a measure to complete the inspection in a shorter amount of time. 2) The under cable refers to the section of cable located under the deck, between the hold-down and the anchorages. 3) Modifying the magnetizer refers to adjustment of the existing magnetizer to fit the diameter of the AW main cable. 4) A crane will be required to lift the magnetizer onto the cable for each panel. 5) Set-up of the system includes attaching the magnetizer, winding the cable and setting up the winch. 6) A panel is defined as the space between two adjacent cable bands. Thus, if a band is removed, the magnetizer will be able to inspect the sections of cable on either side of that band without a second set-up. 7) The time required for the magnetizer to perform the inspection, once set-up is complete, is about 30 minutes for every 20 feet.

4.2.3 Dehumidification

Overview

Dehumidification is a steel wire preservation method which focuses on maintaining a controlled environment in order to significantly retard corrosion. It is also known as a dry-air injection system. According to Bloomstine & Sorensen, this tactic has been employed by the U.S. military to protect assets during long-term storage since the 1950's. They also state that the use of dehumidification for suspension bridges was first implemented on the Little Belt Bridge in Denmark in 1970 (2006). In this trial the goal was to prevent corrosion of the inside of steel box girders as well as the steel wires in the anchorage. The technology has since been developed for use in the main cables of many suspension bridges throughout Europe and Japan. As of 2011, there were 21 suspension bridges in 8 countries using dehumidification systems [Bloomstine, 2011]. In addition, studies have been performed to confirm the ability of dehumidification to effectively prevent corrosion inside the main cables. It has been shown that a significant amount of corrosion will only occur with a relative humidity of 60% or above [Suzumura et al, 2004]. Below 60% the rate of corrosion is much slower, and below 40% corrosion will not initiate. This value has been identified by a number of additional sources [Bloomstine and Sorenson, 2006; Gagnon & Svensson, 2010; *AW 2013 Cable Preservation Report by M&M*]. In addition, a study is currently underway at Columbia University to understand how air moves through the cable environment and thus determine the ability of dehumidification to reach all parts of the cable cross-section. The following paragraphs will describe the three systems needed for dehumidification, case studies and a cost analysis.

Dehumidification System

The main components of a dehumidification system include: the dehumidification plant, injection points and exhaust points. The dehumidification plant manufactures dry air which is blown into the cables at the specific injection points. Exhaust points are used to maintain the proper flow and overpressure inside the sealed cable system. The overpressure prevents infiltration of water at minor imperfections along the exterior of the cable sealing system. A layout is designed for each bridge with the goal of optimizing the locations of the dehumidification plants, injection collars and exhaust points. An example layout for the Little Belt Bridge is shown in figure 22.

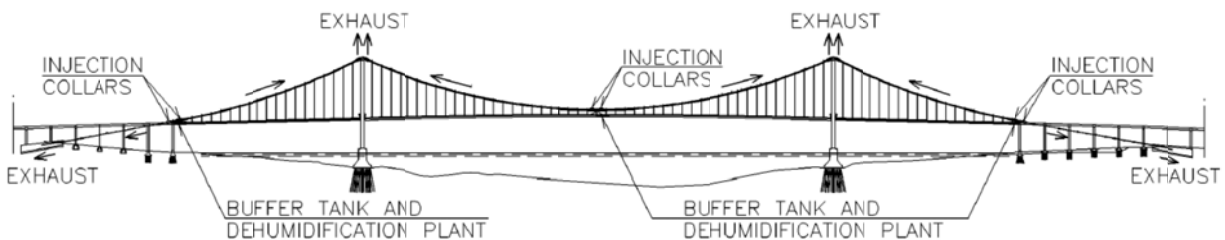


Figure 19: Dehumidification system layout for Little Belt Bridge, Denmark. [Bloomstine & Sorenson 2006]

The dehumidification plant includes the following components: dehumidification unit, a fan, an electrical board, filters and ducting. A complete dehumidification plant can be seen in figure 23. The actual process for drying the air is called active sorption, and is also illustrated in figure 23. A sorbent, or desiccant, is known as a hygroscopic material. An example of a sorbent would be the silica gel packets that can be seen packaged with electronics and carry a warning label which reads "do not eat". These materials can absorb water or return water to the air given the proper environmental conditions and are the key to the dehumidification system. Inside the dehumidification unit is a sorption rotor, or wheel, which is coated with a sorbent. The wheel continuously and slowly rotates through two sides of the rotor chamber. On one side process air is drawn through the rotor, dehumidified, and sent along to the cables. On the opposite side heated air is sent through to rotor and absorbs water from the sorbent material, drying it out. The hot, wet air is then discharged from the system. One optional addition to the plant is a buffer tank. The buffer tank mixes the dried air with some of the ambient air to provide a mixture at the preferred relative humidity. This strategy will reduce the amount of energy consumed through running the dehumidification unit.

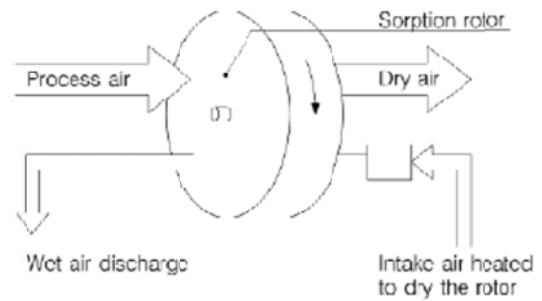
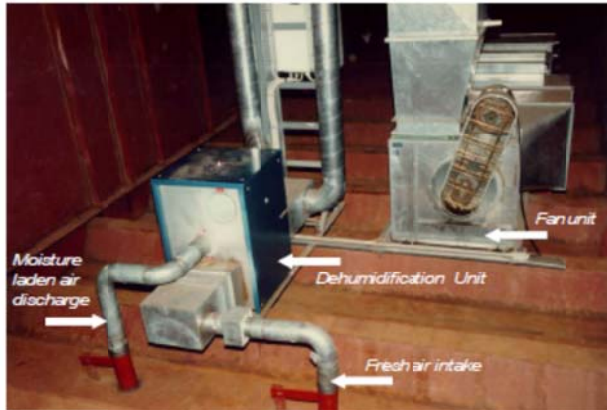


Figure 20: Typical dehumidification plant (left) and diagram of active sorption rotor (right). [Bloomstine 2011]

Sealing System

In most literature, the “traditional” sealing method refers to a combination of galvanized steel wires, zinc paste, wrapping wire and coating of paint to protect the cable. This method has been shown to be inadequate at preventing corrosion on many bridges and, at best, only delaying corrosion on others. In addition, the use of oil or paste is not compatible with the dehumidification since this would interfere with the flow of dry air through the cable. During this research two forms of cable sealing were found which seem to compliment the use of a dehumidification system: an elastomeric wrap aptly named Cableguard™ and a specially designed S-shaped wrapping wire and flexible paint system.

Cableguard™ Elastomeric Cable Wrap System

The recommended system by Bloomstine and Sorenson is the Cableguard™ Elastomeric Cable Wrap System produced by the D.S. Brown Company. The material is an elastomeric wrap manufactured with a thickness of 1.15 mm and a width of 200 mm. During application, the material is wrapped in tension with a 50% overlap resulting in a uniform 2.3 mm thickness. The wrapping process can be seen in figure 24, to the right. The final step in the installation is heat molding. During this process a specially designed blanket heats the material which reacts like a shrink wrap, bonding both layers to create a seal around the cable. The advantages of this product include:

- Able to withstand sufficient overpressure
- Environmentally friendly (no paint products involved)
- Available in numerous colors
- Lack of fumes or blasting during installation
- Installation less sensitive to inclement weather
- Relatively short construction period
- Virtually maintenance free
- UV and weather resistant over lifetime
- Easy to replace



Figure 21: Cableguard™ wrapping application. [dsbrown.com]

S-shaped Wire Wrapping System

Another system identified during literature review is the S-shaped Wire Wrapping System, produced by Tokyo Rope MFG. CO. The S-shaped wire was specifically designed to increase the efficiency of

dehumidification systems. The product is a specially designed wrapping wire with an S shape which is wrapped such that it forms a continuous link along the cable. The linked wire restricts the displacement of the wrapping wire and provides a better surface for painting. The extra rigidity helps to prevent cracks in the paint allowing the exterior of the protection surface to last longer. The S-shaped wire creates higher water sealing and air tightness than the traditional round wire wrapping. The product is typically paired with a specialized, 4 layer, flexible paint system which provides additional protection against cracking and weathering compared to traditional paint. This reduces the maintenance and decreases the frequency of re-painting the cables. Figure 25 shows the cross-section of the S-wire and paint corrosion protection system.

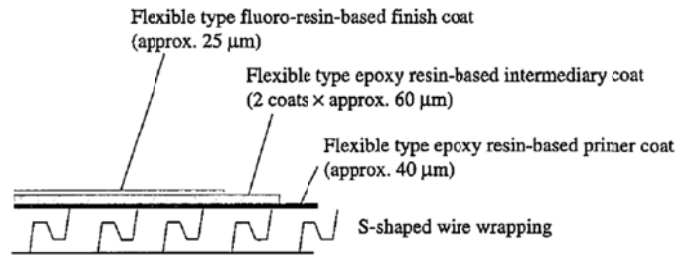


Figure 22: S-shaped wrapping wire and flexible paint corrosion protection systems. [Eguchi et al. 1999]

Monitoring System

The monitoring and control system provides validation that the system is performing as expected as well as provides the ability to adjust the system to reach optimal performance. Instrumentation is placed at key points through the system including the dehumidification plant, the buffer tanks, the injection points and the exhaust points. The instruments monitor functionality, relative humidity, temperature, flow and pressure at each point, where applicable.

Case Studies

Dehumidification has been implemented on a variety of suspension bridges, new and old. The layout of the system on each bridge was designed to utilize existing bridge components and optimize energy consumption. The following are brief summaries of case studies described by [Bloomstine and Sorenson, 2006], and [Bloomstine 2011].

Little Belt Bridge, Denmark

As mentioned above, the Little Belt Bridge was the first bridge to be protected by dehumidification. In 1996 it was determined that the surface paint, the previous protection strategy, was nearly gone. An in depth inspection was performed to identify the best corrosion protection strategy available. The results of that investigation found the optimal solution to be dehumidification combined with a sealing system provided by an elastomeric wrap, Cableguard™. The system has been in place since 2003 had been working very well through 2011, when the reference was written. The layout for this bridge can be seen in figure 21. The monitoring system reports that the relative humidity of the buffer tank and exhaust points are between 40-45% and 35-55% respectively. No leakage has been identified by the monitoring system.

Aquitaine Bridge, France

The Aquitaine Bridge is a suspension bridge with main cables made up with locked coil strands. During the initial construction the wires in these strands were not galvanized and the only corrosion protection was paint. Naturally, as maintenance of the interior strands was impossible, these conditions lead to issues with corrosion. The cables deteriorated quickly and in 1999 they decided to replace the entire cable system. The protection system devised for the new cables included galvanized steel wires in all the strands, galvanized wrapping wire, a dehumidification system and an elastomeric wrap. The dehumidification plants were installed on top of each pylon and the exhaust points are at the low positions of the cable. This system was also completed in 2003 and had been working satisfactorily since. The monitoring system recorded relative humidity at the exhaust points to be approximately 25%. Bloomstine

and Sorenson also suggest that this system could be optimized by changing the target level to something closer to 40%.

Högakusten Bridge, Sweden

The Högakusten Bridge is located in Stockholm, Sweden and opened in 1998. The main cables are made up of parallel wires and are approximately 1,900 m long. The original corrosion protection system included galvanized wires, zinc paste, wrapping wire and paint. In 2004, a window of the cable was opened to inspect the condition of the zinc protection after suspicions arose of accelerated deterioration. The inspection showed ferrous corrosion already occurring on the bottom wires. Later in 2004, a project was initiated to install a new dehumidification system on the bridge. The layout included a buffer tank and dehumidification unit installed at each tower, as well as at mid-span. Exhaust points were installed at the anchorages and the halfway points between the towers and mid-span. Water removal data was collected during the period that the cable was still drying out. Through comparing the water content of the injection and exhaust air, they estimated the system was removing about 1 liter per day from each stretch of cable (310 m). It took about a year and a half for the cable to dry out, removing about 3% of the cable volume worth of water in the process.

General Cost and LCC Analysis

Bloomstine and Sorenson prepared a comparison of the Life Cycle Cost (LCC) of a dehumidification system and the traditional protection system. Unfortunately, this cost comparison was normalized such that the highest cost strategy was indexed as 100, resulting in data that only provides relative cost information. However, this data does provide insight into the relative advantages of dehumidification operation and maintenance costs. The first strategy considered was dehumidification. The costs included for this strategy encompassed the installation and lifetime maintenance for the elastomeric wraps (30 year lifetime), exposed ducts and details (30 year lifetime), the dehumidification system (60 years) and the electrical consumption (< 20,000kWh per year). The second strategy actually considered two options for traditional protection (2 & 2a). The first option (2) assumed a paint lifetime of 20 years, while the second option (2a) assumed a paint lifetime of 30 years. Both options also included spot repairs of the paint system every 5th year of service, for 60 years.

The results of this study showed that installation and maintenance of a dehumidification system over 60 years cost approximately 28% and 16% less than traditional options 2 & 2a, respectively. When considering simply maintenance and operation costs, these savings jump to approximately 56% and 32%, respectively, showing a significantly reduced cost compared to a traditional system. It should also be mentioned that the difference in cable deterioration is not included in this calculation; however, more severe deterioration as a result of using the traditional protection will likely result in higher inspection and rehabilitation costs down the road.

The best quantitative estimate that UT is aware of is the 2013 Cable Preservation Study Report that was prepared by Modjeski & Masters in February, 2013. This study analyzed the cost of three suspension bridges in Great Britain which have recently installed a dehumidification system and the William Preston Lane, Jr. Memorial Bridge, in Maryland, which plans to install a dehumidification system in 2016. The study converted each total cost to the corresponding 2013 costs in U.S. dollars, and then identified a per foot cost for each bridge. The average of these costs was \$885 per foot of cable. They calculate that installing a dehumidification system for the Anthony Wayne the approximate cost would be \$3.5 million. This includes the cost of the Cableguard™ sealing system, which the Department is likely to replace anyway. In this view, the cost of adding the dehumidification system into tentative rehabilitation plans will add only the portion of \$3.5 million not associated with wrapping/sealing the cable.

5.0 Conclusions & Recommendations

5.1 Summary of Current Condition

The recent invasive inspection did not collect enough statistically significant data. Modjeski & Masters (M&M) mentioned that the minimum number of panels to be inspected during the first opening, as recommended by the NCHRP Report 534, is six panels. When compared to only four openings, it should be assumed that this adds some amount of error to the calculated cable strength, in addition to the error intrinsically associated with assumptions made during this type of procedure. However, the NCHRP Report 534 also recommends that the first invasive inspection occur at the age of 30 years old. Conditions for additional inspections require higher number of panels based on the amount of stage 3 and 4 corrosion found during the previous inspection. As an 82 year old bridge, the number of panels required to gain the statistical significance recommended by the NCHRP Report 534, and therefore validate the use of their strength calculations, would have been 6 to 12 panels per cable. The recent inspection resulted in a calculated factor of safety of 2.41 and is estimated to reach 2.15 by 2025. The inspection of additional panels and analysis of the ductility of the wires might produce an increase in expected cable strength, and the rate of cable decay, through the use of the limited ductility method. No evidence of wire breaks was found during the invasive inspection. In addition, no wire breaks have yet to be recorded by the acoustic monitoring system, which has been operating since 2011. Considering this, it is possible the cable is in better condition than the data is able to suggest.

The limited ductility method could not be used to calculate cable strength in the M&M report because the ultimate strain of wire specimens was not recorded. If the ultimate strain were estimated based on the ultimate strength, assuming the strain-strain curve is linear from the last recorded point, it would be possible to project a rough estimate of calculated cable strength using the limited ductility method. This would require the bold assumption that the ductility shown in the specimens taken from the four locations are representative of the conditions of the wires throughout the entire cable. This technique would provide some idea of what could be expected if additional panels were inspected, as recommended by M&M.

5.2 Rehabilitation and Advanced Inspection Cost vs. Reliability Estimates

During the project review session, the technical panel presented an interest in identifying the reliability associated with potential monitoring and preservation technologies. In short, if certain measures are taken, what level of confidence is there that the bridge will be in the condition expected? This is an intrinsically difficult question to answer, and typically involves a level of statistical probability which is out of the scope of this project. However, reliability is a measure which requires a minimum amount of statistically significant field data to determine. The best way to improve overall confidence in the reliability of cable health into the future, regardless of additional monitoring or preservation techniques, is to obtain a comprehensive understanding of the current state of the AW main cable.

The question is cost vs. increase in reliability or increase in certainty of the reliability estimate. This is an insightful question that is beyond the state-of-the-art. However, answering this question is in the wind. The authors are reviewing some proposals to initiate work into investigating this topic. The leader in this work is Daniel Frangpol at the Lehigh; however, no work has advanced to the point of comparing reliability to cost. The present state of the art is developing estimates of reliability based on field data and changes in reliability with respect to time based on field data. The authors will continue to investigate this topic during the review of this draft report.

5.3 Best Practices Recommendation for the Anthony Wayne

As mentioned above, the best way to increase reliability of monitoring and preservation strategies into the future is to gain a comprehensive understanding of the current condition of the cable. Monitoring strategies can only provide a limited amount of confidence without a good baseline. A base line could be established utilizing invasive inspection or non-invasive inspection in the form of the magnetic main flux method. Based on the opinions of several distinguished suspension bridge experts, the most reliable action would be to wedge the entire length of the cable during the cable re-wrap project in 2016. An

inspection can be performed following the NCHRP Report 534 guidelines with samples taken only from the worst locations found along the cable.

With an established baseline, the wire break monitoring provides a great tool for tracking future deterioration of the cable through wire breaks. Over the long term, this strategy should be continued and coupled with periodic invasive inspections of the cable.

Installing a dehumidification system is the best long term cable preservation technique available. This system will provide the highest level of confidence in slowing the deterioration due to corrosion. The system has the capability of preventing infiltration of water into the cable by maintaining a minimum overpressure. Installation of a dehumidification system would reduce the required frequency of invasive inspections.

Internal sensors would compliment both continued corrosion monitoring research and the installation of a dehumidification system. Installation of internal sensors would be most useful if installed at two locations; the worst cable location identified, and one of the better cable locations for comparison. In this way the corrosion rate of the worst section could be monitored. Internal sensors would also validate the effectiveness of a dehumidification system to lower relative humidity throughout the entire cross-section of the cable. It is recommended that allow laboratory testing as a part of future research prior to potential installation during the cable rehabilitation in 2016.

5.4 Future Research

While the attempts in this study to practically detect corrosion using the current AE system were unsuccessful, the investigators are not convinced that this cannot be done. Corrosion experiments in the laboratory setting show corrosion, given the right conditions, to be quite detectable. The low frequency sensor, R.45, proved to be much more suited to corrosion detection than the all-purpose R15 α . During corrosion of galvanized wires, corrosion was not only detectable but abundant, with amplitudes reaching as high as 82 dB. The lack of attenuation along the steel bar is also promising. In fact, through the application testing from this study, the team simply identified several methods of how not to detect corrosion at the cable bands. More importantly, however, the results have helped to identify additional methods to improve the quality of corrosion testing & monitoring. Modifications and opportunities for potential future research include:

- Improved attenuation and filter studies through the use of more accurate wire to cast iron bar interface to simulate the cable band.
- Modification and refinement of graphical corrosion filter. One possible waveform feature which may help distinguish corrosion from other sources of AE is the signal envelope.
- Experience will improve future field testing through improved methods for attaching a corrosion cell and AE sensor to the cable band.
- Potential future laboratory testing and use of internal sensor would compliment corrosion monitoring research.
- The closure of the AW over the next two years provides a unique opportunity to have more frequent access to lowering the threshold during periods of interest.
- Estimating the effect of rehabilitation and inspection on reliability and factor of safety.

The understanding and foundation built through this project should translate into a more effective experimental program. Combined with opportunities related to the bridge closure and potential internal sensors, future corrosion studies should produce more definitive results. It is recommended that ODOT allow this research to continue through an additional student study contract.

6.0 Recommendations for Implementation of Research Findings

A full length invasive inspection would be performed in conjunction with the cable rehabilitation work already planned. Combining these two activities will likely include substantial cost savings from the \$5,200/foot which was average cost of a standalone cable inspection as determine by M&M in the 2013 Cable Preservation Report. The process of wedging the cable would likely add some time to the project. Having wedged the full length of the cable, ODOT will gain significant confidence in the condition of the cable. Additional wire samples should be taken for testing in order to determine if the limited ductility method can be used by examining the ultimate wire strain. This will likely provide cost savings in the form of less frequent invasive inspections for the remaining life of the cable. The recommended interval of inspections for the NCHRP Report 534 is every 10 years, based on the condition of the cable. Based on the cost figure from M&M, if six panels are inspected per cable, the cost is \$1.25 M per inspection. It is possible the frequency of inspection may be reduced by half or more if a full length inspection is coupled with Dehumidification. Future cost savings and a substantial increase in reliability may justify increased upfront costs.

Installation of a dehumidification will require some investigation into the flow capacity and flow lengths of the cable. Any residual paste that may remain in the cable will hinder the flow of dry air through the bundle. In preparation for a dehumidification system, the wedging of the cable would also provide assurance that there is no such blockage. Eventually, the department will need to design a dehumidification system layout, such as the one shown in figure 22. One of the more challenging aspects to this implementation might be in determining the proper location of the dehumidification plants and buffer tanks; however, how many and the most beneficial location will depend on the flow lengths determined for the cable. It should be noted that as the target of dehumidification is to virtually prevent corrosion, the new driving mechanisms for aging of the AW would likely be fatigue and loss of ductility of the wires. This should be taken into consideration in the selection of monitoring techniques. For this reason it is recommended that ODOT continue to monitor wire breaks with the Acoustic Monitoring system. This system will continue to serve as a warning of potential issues as the cable continues to age.

Application of an internal sensor system to the AW would also occur during the cable rehabilitation project in 2016. The sensor system would provide additional validation for the potential dehumidification system and corrosion monitoring research. A section on internal sensor testing will be included in the proposal for future research mentioned below. Mistras Group was part of the project at Columbia which designed and implemented the internal sensor package. Therefore, connecting the sensors to the existing SHII data acquisition system should not be an issue. It can be expected that the cost for sensor hardware would be approximately \$1000 per location, not including additional cables or software/hardware upgrades for the DAQ.

The primary investigator will submit a separate proposal outlining future research, describing the impacts on all the work to be completed on the Anthony Wayne in the near future.

7.0 Bibliography

Barton, S. C., Vermaas, G. W., DUBY, P. F., West, A. C., & Betti, R. (2000). "Accelerated corrosion and embrittlement of high-strength bridge wire." *Journal of materials in civil engineering*, 12(1), 33-38.

Bloomstine, M. L., & Sørensen, O. (2006). "Prevention of main cable corrosion by dehumidification." *Advances in Cable-supported Bridges*, 215.

Bloomstine, Matthew L. (2011). "Main Cable Corrosion Protection by Dehumidification—Experience, Optimization and New Development." *Modern Techniques in Bridge Engineering*: 39.

Cao, Y., Vermaas, G. W., Betti, R., West, A. C., & DUBY, P. F. (2003). "Corrosion and degradation of high-strength steel bridge wire." *Corrosion*, 59(6), 547-554.

D.S. Brown. "CABLEGUARD Elastomeric Cable Wrap System," <http://www.dsbrown.com/Resources/Bridges/cableguard/cableguard_brochure_2013v4.pdf>, September 15th, 2013.

Eguchi, T., Suzumura, K., Matsuoka, T., Watanabe, T., Miwa, K., Sasaki, N., & Seiryu, M. (1999). "Development of Corrosion Protection Methods Using S-shaped Wire Wrapping System." *Shinnittetsu Giho*, 8-14.

Elliott, J., Paulson, P., & Youdan, D. (2001). "The Use of an Acoustic Monitoring System to Confirm the Integrity of Tensioned Steel Elements." Pure Technologies Ltd, Calgary, Alberta, Canada. *Evaluation of Suspension Bridge Parallel Wire Cables*. Transportation Research Board,

Fregonese, M., Idrissi, H., Mazille, H., Renaud, L., & Cetre, Y. (2001). "Initiation and propagation steps in pitting corrosion of austenitic stainless steels: monitoring by acoustic emission." *Corrosion Science*, 43(4), 627-641.

Gagnon, C. & Svensson, J.. (2010). "Suspension bridge cable evaluation and maintenance." 2010 IABSE-JSCE Joint Conference on Advances in Bridge Engineering-II, Bangladesh group of the International Association for Bridges and Structural Engineers, Dhaka, Bangladesh.

Gostautas, R., Nims, D., Tamutus, T., Syedianchoobi, R. (2012). "Acoustic Monitoring of the Main Cables of the Anthony Wayne Suspension Bridge." *Structural Materials Technology Conference (SMT): NDE/NDT for Highways and Bridges*, The American Society for Nondestructive Testing, Inc. (ASNT), Columbus, OH, 111-119.

Higgins, M. S. (2006). "Health Monitoring Combined with Visual Inspections- Obtaining a Comprehensive Assessment of Cables." Pure Technologies Ltd, Columbia, MD.

Kasai, N., Park, S., Utatsu, K., Sekine, K., Kitsukawa, S., Mitsuta, T. (2008). DRAFT: "Evaluation of the Corrosion Rate for Acidic Bottom Plates of an Aboveground Oil Tank by the AE Method." 2008 ASME Pressure Vessels and Piping Division Conference, The American Society of Mechanical Engineers (ASME), Chicago, Illinois, USA.

Kele Precision Manufacturing. "Data Sheet for HS-2000v RH & Temperature Sensor," http://www.precounusa.com/humidity_moisture_dew_sensors.htm, September 15th, 2013.

Khazem, D., Serzan, K., & Betti, R. (2012). "Remote Monitoring of Suspension Bridge Cables as Calibrated in the Laboratory and Tested in the Field." *Bridge Maintenance, Safety, Management, Resilience and Sustainability*, Taylor & Francis Group, London, England.

Lee, C. K., Scholey, J. J., Worthington, S. E., Wilcox, P. D., Wisnom, M. R., Friswell, M. I., & Drinkwater, B. W. (2008). "Acoustic emission from pitting corrosion in stressed stainless steel plate." *Corrosion Engineering, Science and Technology*, 43(1), 54-63.

Maybaurl, R. M. and Camo, S., *NCHRP Report 534: Guidelines for Inspection and Strength*

Mazille, H., Rothea, R., & Tronel, C. (1995). "An acoustic emission technique for monitoring pitting corrosion of austenitic stainless steels." *Corrosion Science*, 37(9), 1365-1375.

Petroski, H. (2006). Engineering Waldo-Hancock Bridge. *American scientist*, 94(6), 498-501.

Pollock, A. A. (1986). "Acoustic emission capabilities and applications in monitoring corrosion." *Corrosion Monitoring in Industrial Plants Using Nondestructive Testing and Electrochemical Methods*, 30-42.
Pure Technologies LTD, (2004), "Waldo Hancock Bridge, Verona, Maine", Project Fact Sheet

Roberge PR., (2006), "Corrosion Electrochemistry," *Corrosion Basics—An Introduction*, 2nd ed. Houston, Texas: NACE International, 2006.

Sloane, M., Betti, R., Marconi, G., Hong, A. H., & Khazem, D. (2012). "Main Cable Corrosion Monitoring for Suspension Bridges Using a Nondestructive Sensing System." *Structural Materials Technology Conference (SMT): NDE/NDT for Highways and Bridges*, The American Society for Nondestructive Testing, Inc. (ASNT), Columbus, OH, 321-329.

Sloane, M., Betti, R., Marconi, G., Hong, A. H., & Khazem, D. (2012). "An Experimental Analysis of a Non-Destructive Corrosion Monitoring System for Main Cables of Suspension Bridges." *Journal of Bridge Engineering*; Accepted manuscript, not copyedited.

Sugahara, M., Kai, Y., Tsukada, K. (2012). "Nondestructive Evaluation of Bridge Cables and Strands Using the Magnetic Main Flux Method (MMFM)." *Structural Materials Technology Conference (SMT): NDE/NDT for Highways and Bridges*, The American Society for Nondestructive Testing, Inc. (ASNT), Columbus, OH, 111-119.

Suzumura, K., & Nakamura, S. I. (2004). "Environmental factors affecting corrosion of galvanized steel wires." *Journal of Materials in Civil Engineering*, 16(1), 1-7.

The Anthony Wayne Bridge over the Maumee River: 2013 Cable Preservation Study Report for the Ohio Department of Transportation, prepared by Modjeski and Masters, Inc. for ARCADIS, 2013.

The Anthony Wayne Bridge over the Maumee River: 2013 Cable Strength Evaluation Report for the Ohio Department of Transportation, prepared by Modjeski and Masters, Inc. for ARCADIS, 2013.

Wang, G., Lee, M., Serratella, C., Botten, S., Ternowchek, S., Ozevin, D., ... & Scott, R. (2010). "Testing of acoustic emission technology to detect cracks and corrosion in the marine environment". *Journal of Ship Production and Design*, 26(2), 106-110.
Washington, D.C., 2004.

Yuyama, S., & Kishi, T. (1983). AE analysis during corrosion, stress corrosion cracking and corrosion fatigue processes. *J. Acoust. Emiss.:(United States)*, 2.

Yuyama, S., & Nishida, T. (2002). "Acoustic emission evaluation of corrosion damages in buried pipes of refinery." *Progress in Acoustic Emission*, 11, 197-204.

Appendices

Appendix A: Sample Data Sheets from Corrosion Testing

Appendix B: Internal Sensors Product Specifications

Appendix C: Quote from CTNA for MMFM Inspection of AW

Appendix A:

Sample Data Sheets from Corrosion Testing

*Note: all data collected and presented in this report is stored on a disk. This information can be made available if required. The following forms are samples of the Experimental Set-up Data Sheet (shown below) and Experimental Analysis Data Collection Sheet (next page) respectively.

C4-G-RS3-3		Date	
		Data file name	
General Information			
Channel #1	R15α	Channel #2	R.45
Experiment Start Time		Experiment Corrosion Time (hrs)	
Experiment End Time		Cumulative Cell Corrosion Time (hrs)	
Hardware Setup for Corrosion Layout on Pocket AE			
Timing		Standard	
Maximum Duration (ms)	3	Threshold (dB)	45
PDT (us)	500	Pre-Amp	Internal
HDT (us)	800	Sample Rate	5MSPS
HLT (us)	1000	Lower Frequency (kHz)	20
		Upper Frequency (kHz)	300
Hit Set		Waveform	
Amplitude	Risetime	Pre-Trigger	64
Energy	Avg. Frequency	Length	15k
Counts			
Duration			
ASL			
General Description of Experiment			
Comments & Observations			
Pictures (left: before; right: after)			

Data Collection Sheet			
Name of File:		Phase:	
Ranges of Parameters			
Minimum and Maximum for Channel 1 (High Frequency Sensor, R15 α)			
Amplitude	Duration	Rise Time	Avg. Frequency
Minimum and Maximum for Channel 2 (Low Frequency Sensor, R.40)			
Amplitude	Duration	Rise Time	Avg. Frequency
Length of Test	Number of Hits that are within filter settings		
	Duration (us)	Rise Time (us)	Avg. Frequency (kHz)
Low Frequency Sensor (R.40)	0 to 800	0 to 400	10 to 200
High Frequency Sensor (R15a)	0 to 800	0 to 400	10 to 200
	Channel 1 (R.40)	Channel 2 (R15 α)	Total Hits
Number of Hits			
Average Hit Rate (Hits vs. time)			
	First Slope	Second Slope	Third Slope
Channel 1 (High Frequency)			
Channel 2 (Low Frequency)			
Shape of Hits vs. Time Curve			
Low Frequency		High Frequency	
Test Conditions			
Continuous corrosion		Non-continuous corrosion	
Submerged cell		Wet cell	
Additional Comments			

Appendix B:

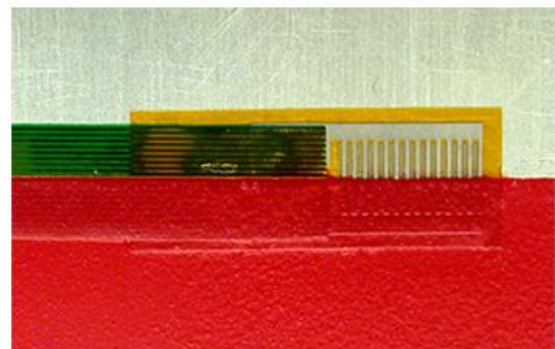
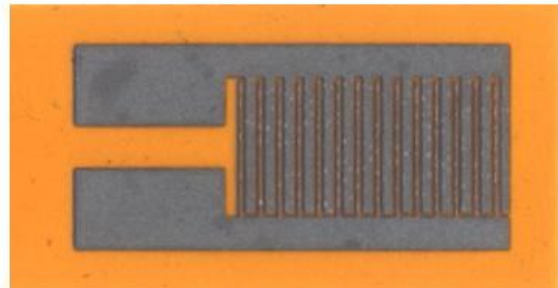
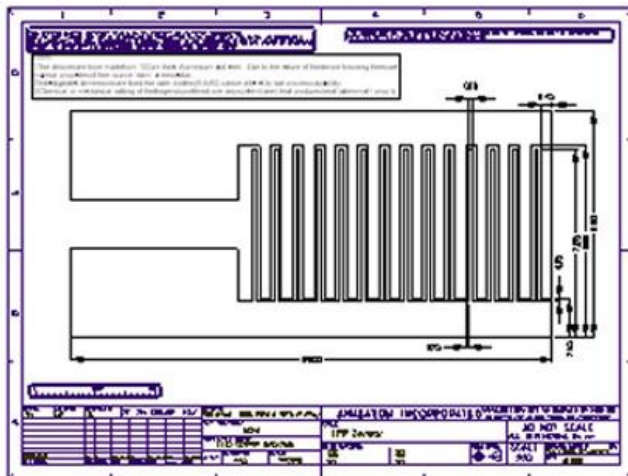
Internal Sensors Product Specifications

Analatom Linear Polarization Resistance (LPR) sensor information:

Analatom Sensor System Technical Specifications					
Specification	Value	Units	Specification	Value	Units
Temperature			Voltage		
min	-40	°C	min	2.7	volts
max	85	°C	max	3.4	volts
Data Transfer			Data Storage		
download speed (RS-232)	4,800	baud	size	1,048,576	bytes
download speed (ZigBee)	115,200	baud	number of measurements	24,900	---
Current Drain			External Sensors		
data download (RS-232)	3	mA	A/D channels for external sensors	4	---
data download (ZigBee)	45	mA	Detectable Corrosion Rates (304 Steel)		
data measurement between measurements	1	mA	min	0.0001	mm/year
with 802.11b module	500	mA	max	10	mm/year

Source: <http://www.analatom.com/system.html>

Linear Polarization Resistance (LPR) Sensor



Application Notes

1. Stabilization Period: The HS-2000V requires a stabilization period of up to 5 minutes upon powering up the sensor. This is primarily due to the slew rate of the output circuit. When the sensor is first powered up it will read near zero volts. After a short period (less than 15 seconds), the sensor output will begin to increase. Since the output is slew rate limited, the final stabilization time will depend on the ambient conditions. The longest stabilization is required when the ambient parameter, either temperature or humidity, is near full scale (130 degrees C or 100% RH respectively) since these will generate output voltages near the supply voltage.

2. Temperature Output: The temperature output is ratiometric over the range of -22° to 212°F (-30°F to 100°C) for the HS-2000V. Note: Accuracy published within recommended operating temperature.

3. PCB Connectors: It is recommended that HS-2000V be socketed rather than soldered to circuit boards. If a direct solder connection is required, it is recommended that hand-soldering be performed using a rosin-based flux. The soldered surfaces may be cleaned with isopropyl alcohol (do not immerse). The recommended PCB sockets include:

Surface Mount:

- Mill-Max: 310-93-104-41-105, 4 pin SMT, Left hand footprint, 30 micro inch gold plate
 - Mill-Max: 310-93-104-41-107, 4 pin SMT, Right hand footprint, 30 micro inch gold plate
- These sockets are available from Digi-Key in 64 pin strips. See part number ED23064-ND*

Through hole:

- Mill-Max: 310-93-104-41-001, 4 pin standard solder tail, 30 micro inch gold plate
- These sockets are available from Digi-Key in 63 pin strips. See part number ED7063-ND*

4. Chemical Resistance: Contact Precon for data on resistance to specific chemicals and environments.

Warranty

WARRANTY: The Seller warrants that Warranted Goods shall not fail to function in accordance with the seller's specifications because of defects in material or workmanship, for one year from the date of purchase. The foregoing warranty is expressly in lieu of all other warranties, express or implied, including warranties of merchantability or fitness for a particular purpose, or any other matter with respect to the goods are excluded and shall not apply to the goods sold. The warranty undertaking in this agreement does not apply to any goods that have been subjected to accident, disaster, loss or damage during shipment, neglect, misuse, improper installation, corrosive atmosphere harmful to electronic circuitry, excessive electromagnetic fields, failure or insufficiency of electrical power or unusual electrical surge or shock, nor to dysfunction or malfunction of, or caused by, any other equipment or device (other than equipment or devices you have purchased from us) to or in which such goods have been attached or installed.

Seller's employees, agents and/or representatives may have made oral statements about the goods sold or to be sold. Such statements DO NOT constitute warranties and ARE NOT part of a sales Contract. Seller's liability to Buyer, their agents, employees, customers, assigns, successor or other related parties for any and all losses or damages resulting from Seller's breach of a sales Contract, whether in tort or in contract or otherwise, shall be limited to the replacement of a like quantity of goods sold and IN NO EVENT SHALL SELLER BE LIABLE FOR SPECIAL, INDIRECT, INCIDENTAL, CONSEQUENTIAL, OR CONTINGENT DAMAGES (including, without limitation, loss of anticipated profits, business interruption, loss or use or revenue, litigation costs, cost of capital, Buyer's fixed costs, or avoidable costs).

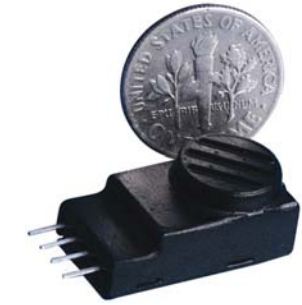
All specifications are subject to change without notice. For the latest specifications, visit our website at www.preconusa.com

The innovative HS-2000V Humidity Sensor combines capacitive-polymer sensing technology with a novel measurement method, eliminating the need for temperature correction and calibration by the user. The sensor, which is calibrated at Precon before shipment, includes a thermistor and circuitry to correct for temperature and calculate the true relative humidity. The sensor provides both humidity and temperature outputs and is accurate to ±2%.

The output of the HS-2000V is ratiometric, with the output voltage varying from zero to the supply voltage as the measured parameter varies from zero to full-scale. For example, at a supply voltage of 5.0 volts, 50% RH produces a 2.5 volt output signal on the RH output pin.

The HS-2000V may be applied within an environmental operating temperature range of 32° to 158°F (0° to 70°C). The temperature output range is -22° to 212°F (-30° to 100°C), linear from 0 VDC to power supply voltage.

The four-pin connection provides for easy installation or replacement in the field, reducing the overall cost to maintain large or complex systems.



Features

- RH & Temperature Outputs
- Temperature Compensated
- Factory Calibrated
- Accurate to ± 2%
- Field Replaceable
- Good Stability
- Excellent Chemical Resistance
- Analog Voltage Output
- Low Cost

Typical Applications

- OEM Equipment • Medical
- HVAC • Pharmaceutical
- Computer Rooms • Industrial
- Critical Space Monitoring
- Food Equipment
- Humidifiers • Data Logging
- Automation • Refrigeration
- Environmental Chambers
- Laboratory • Clean Rooms

MAXIMUM RATINGS

- Operating Temperature .. 32° to 158°F (0° to +70°C)
- Temperature Output Range -22° to 212°F (-30° to 100°C)
- Storage Temperature 22° to 257°F (-40° to +125°C)
- Operating Humidity Range 0-100 percent
- Supply Voltage +5.5 volts
- Soldering Temperature..... 10 sec at 520°F (250°C)

SPECIFICATIONS

Humidity

Accuracy..... $\pm 2.0\%$ RH typical, 0-100% non-condensing (Note 1)
 Linearity..... $\pm 0.5\%$ RH
 Hysteresis..... $\pm 1.0\%$ RH , maximum
 Temperature Coefficient..... $\pm 0.008\%$ RH / °C, maximum
 Response Time 25 sec. in slow moving air at 77°F (25°C)
 Recovery Time (from condensation) 10 seconds
 Stability..... $\pm 0.5\%$ RH / year
 RH Voltage Output..... Ratiometric: 0 VDC to Supply voltage corresponds to 0% to 100% RH

Temperature

Accuracy..... $\pm 0.40^\circ\text{C}$ Typical (Note 2)
 Temperature Voltage Output..... Ratiometric: 0 VDC to Supply voltage corresponds to -22° to 212°F (-30° to +100°C)
 Response Time..... 50 sec. in slow moving air

General

Power Requirements...
 Voltage Supply..... 2.0 – 5.5 VDC, 32° to 158°F (0° to 70°C)
 Operating Current..... 1.5 mA, maximum (Note 3)
 1.2 mA, typical
 Output Slew Rate..... 0.015 volt / second (Note 4)
 Load Impedance..... 50,000 ohms minimum (Note 5)
 Package..... Four pin SIP with 0.100 inch lead spacing
 Handling..... ESD >4 KV, Human Body Model

PIN DIAGRAM

(Front View)



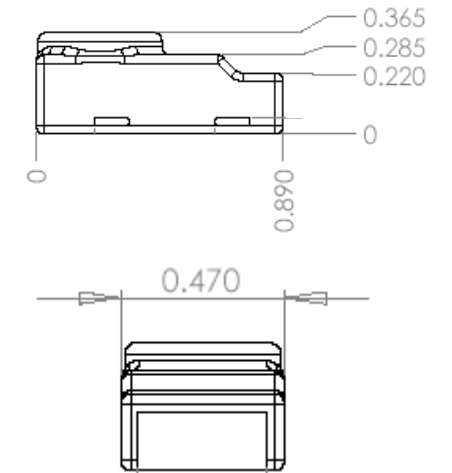
Pin # 1 2 3 4

Pin 1	Temperature Out (0 to Vsupply)
Pin 2	Power (2 to 5.5 volt)
Pin 3	RH Out (0 to Vsupply)
Pin 4	Ground

Notes:

1. See Figure 1 on page 3
2. See Figure 2 on page 3
3. Supply voltage equals 5 volts. Does not include current supplied to loads connected to temperature and relative humidity outputs
4. For a discussion on slew rate, see Application Note #1 on page 4.
5. For loads between 1k to 50k, contact factory.

Dimensions



Tolerance on all dimensions ± 0.005 inch

Ordering Information

MODEL NUMBER	DESCRIPTION
HS-2000V	Relative humidity and temperature sensor: Analog voltage output; RH range: 0 to 100%; Operating temperature range: 32° to 158°F (0° +70°C) Output temperature range: -22° to 212°F (-30° +100°C) NOTE: Accuracy published within recommended operating temperature.

FIG. 1 RH ACCURACY

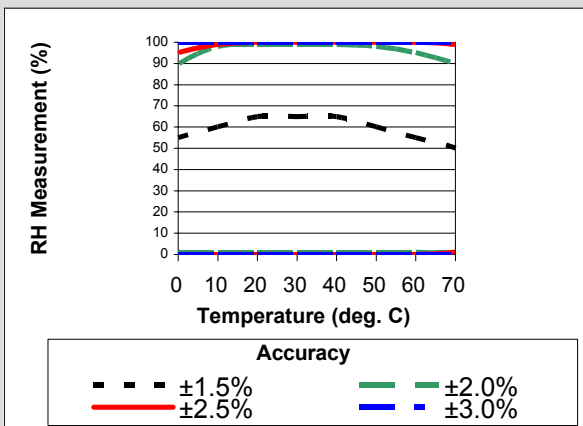
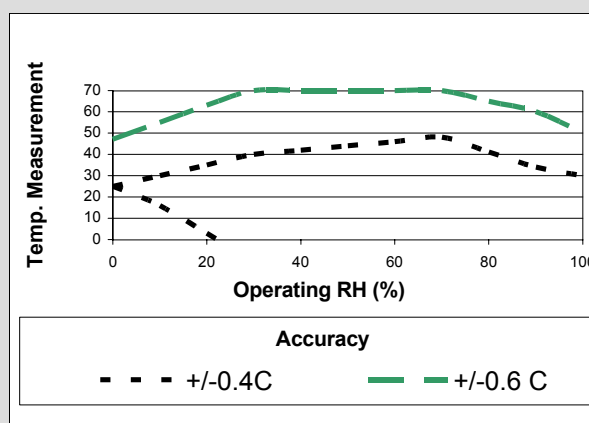


FIG. 2 TEMPERATURE ACCURACY



Appendix C:

Quote from CTNA for MMFM Inspection of AW

OPTION-01

Number of measurement location	Typical panel parts	4 panels
	Under cable parts	0 location
Number of using magnetizer		1 set

Item	Subtotal		
1. Labor Cost	41,180		
2. Travel Fee	4,902		
3. Inspection Fee	39,916		
4. Equipment Fee	93,500		
Total	179,498		

QUOTATION

Task Description	Supervisor Hours	Engineer Hours	Technician Hours
1. Preparation of equipment at facility	16.0	16.0	
2. Mobilization Transfer to Toledo Unpacking and setting of the equipment	12.0	12.0	
3. Magnetic measurement work at site Typical panel parts 4 days x 10hours Under cable parts	40.0 0.0	40.0 0.0	
4. Demobilization Packing and loading Transfer back home	12.0	12.0	
5. Over work extra (24 hours x 0.5 = 12 hours)	12.0	12.0	
6. Clean up at facility Unloading and cleaning up of the equipment at facility	8.0	8.0	
7. Report	40.0		
Total Hours	140.0	100.0	0.0
Labor Rates (per hour)	\$ 187.00	\$ 150.00	\$ -
Labor cost	\$ 26,180	\$ 15,000	\$ -
Labor Subtotal	\$ 26,180	\$ 15,000	\$ -
Total cost of Labor	\$ 41,180		

Travel	Unit	Quantity	Unit Cost	Total Cost
Per Diem 6 days x 2 persons	day	12	\$ 45	\$ 540
Hotel 5 night x 2 persons	night	10	\$ 125	\$ 1,250
Mileage 200 miles x 1 time (Novi ⇄ Toledo)	miles	200	\$ 0.56	\$ 112
Airfare (1 engineer from Japan)	trip	1	\$ 3,000	\$ 3,000
			\$ -	\$ -
			\$ -	\$ -
			\$ -	\$ -
Total cost of Travel				\$ 4,902

Inspection Fee	Total Cost
Inspection Fee	\$ 39,916

Equipment fee	Unit	Quantity	Unit Cost	Total Cost
Modifying fee of magnetizer	set	1	\$ 20,000	\$ 20,000
Production fee of jigs	set	1	\$ 30,000	\$ 30,000
Transportation fee of equipment(from Japan)	each	1	\$ 35,000	\$ 35,000
Depreciation fee of equipment (Wear and Tear Fee)	each	1	\$ 7,500	\$ 7,500
Miscellaneous	each	1	\$ 1,000	\$ 1,000
				\$ 93,500

Total Cost \$ **179,498**

OPTION-05

Number of measurement location	Typical panel parts	4 panels
	Under cable parts	4 location
Number of using magnetizer		1 set

Item	Subtotal		
1. Labor Cost	68,140		
2. Travel Fee	7,345		
3. Inspection Fee	62,597		
4. Equipment Fee	105,500		
Total	243,582		

QUOTATION

Task Description	Supervisor Hours	Engineer Hours	Technician Hours
1. Preparation of equipment at facility	16.0	16.0	
2. Mobilization Transfer to Toledo Unpacking and setting of the equipment	12.0	12.0	
3. Magnetic measurement work at site Typical panel parts 4 days x 10hours Under cable parts 8days x 10hours	40.0 80.0	40.0 80.0	
4. Demobilization Packing and loading Transfer back home	12.0	12.0	
5. Over work extra (24 hours x 0.5 = 12 hours)	12.0	12.0	
6. Clean up at facility Unloading and cleaning up of the equipment at facility	8.0	8.0	
7. Report	40.0		
Total Hours	220.0	180.0	0.0
Labor Rates (per hour)	\$ 187.00	\$ 150.00	\$ 100.00
Labor cost	\$ 41,140	\$ 27,000	\$ -
Labor Subtotal	\$ 41,140	\$ 27,000	\$ -
Total cost of Labor	\$ 68,140		

Travel	Unit	Quantity	Unit Cost	Total Cost
Per Diem 14 days x 2 persons	day	28	\$ 45	\$ 1,260
Hotel 11 night x 2 persons	night	22	\$ 125	\$ 2,750
Mileage 200 miles x 3 time (Novi ⇄ Toledo)	miles	600	\$ 0.56	\$ 335
Airfare (1 engineer from Japan)	trip	1	\$ 3,000	\$ 3,000
			\$ -	\$ -
			\$ -	\$ -
			\$ -	\$ -
Total cost of Travel				\$ 7,345

Inspection Fee	Total Cost
Inspection Fee	\$ 62,597

Equipment fee

Modifying fee of magnetizer	set	1	\$ 20,000	\$ 20,000
Production fee of jigs	set	1	\$ 30,000	\$ 30,000
Production fee of jigs for under cable part	set	1	\$ 10,000	\$ 10,000
Transportation fee of equipment(from Japan)	each	1	\$ 35,000	\$ 35,000
Depreciation fee of equipment (Wear and Tear Fee)	each	1	\$ 7,500	\$ 7,500
Miscellaneous	each	1	\$ 3,000	\$ 3,000
				\$ 105,500

Total Cost \$ **243,582**

